Mullard

Technical Communications

Volume 13 Number 125 January 1975

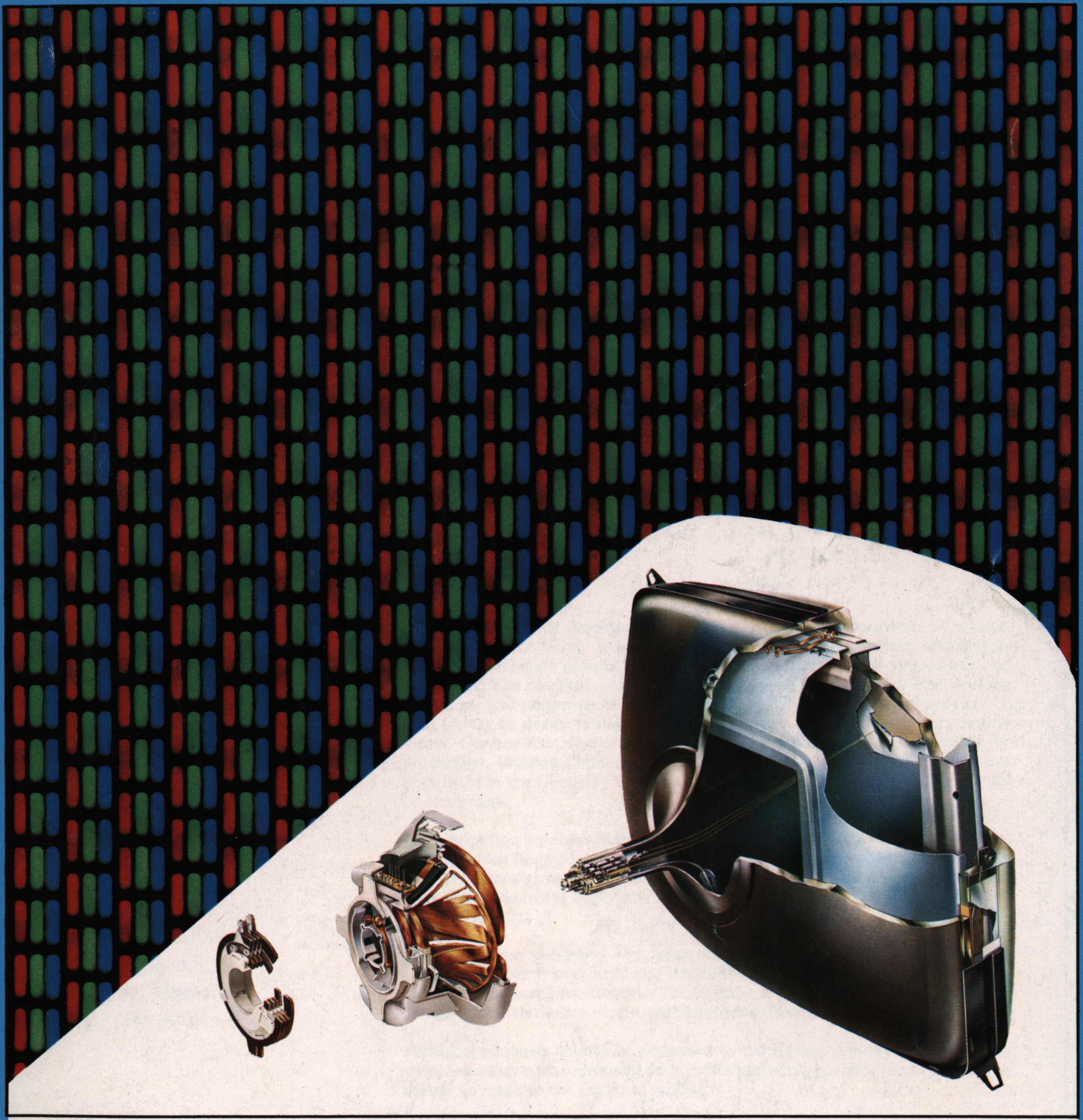

- 20AX 110° colour television: a brief outline
- Full-wave thyristor power supply for television receivers
- Flyback converters with current transformer drive
- FX3700 series transformer cores

Mullard Technical
Communications
ISSN 0027—3139

Volume 13 Number 125 January 1975

Cover Picture:
20AX 110° colour television system: the cutaway shows the picture tube, deflection yoke, and static correction assembly. A magnified view of the screen showing excited phosphor stripes and the shadow of the vertically-slotted mask with its horizontal strengthening bridges is seen in the background.

20AX 110° colour television: a brief outline
M. J. Prescott 186

Full-wave thyristor power supply for television receivers
R. E. F. Bugg 198

Flyback converters with current transformer drive
J. R. Kinghorn 210

Product Information: FX3700 series transformer cores and coil formers for SMPS 225

Editor:
Edmund G. Evans

Assistant Editor:
Michael J. Prescott

Design and Production:
Michael J. Rose

Central Technical Services,
Mullard Limited,
New Road, Mitcham,
Surrey, CR4 4XY

Made and Printed in England by
Wightman & Company Ltd.,
Cranmer Road, London, SW9 6EJ

This journal records developments in the application of electronics in science, industry, and the home. It contains information on the properties and performance of solid-state devices, valves and tubes, and associated components and assemblies. The practical circuits given are designed to provide the best working conditions and performance for the devices used. The design principles may be used (so far as device ratings allow) for adaptation to meet particular requirements. Current data should be consulted before any circuit is considered for production. Mullard Limited can normally supply only those devices or assemblies listed in the Company's current catalogues. Availability in quantity should be confirmed.

All information is published in good faith, but because of the wide variety of situations in which this information may be used, we cannot accept any responsibility for loss or damage resulting from unsatisfactory performance. Publication of this information does not imply any authority or licence for the utilisation of any patented feature.

Four issues are published each year and issued free of charge to equipment designers, research organisations, laboratories, libraries, educational establishments, and consultants. Requests for addition to the mailing list must be made on the official stationery of the establishment concerned.

Technical enquiries should be addressed to the Editor. Abstracts or references should mention both source and authors. Requests for republication or translation should be made to the Editor in writing.

'Mullard' is the trade mark of Mullard Limited and is registered in most of the principal countries of the world.

Mullard Limited, Mullard House, Torrington Place, London, WC1E 7HD Tel: 01-580 6633 Telex: 264341

20AX 110° colour television: a brief outline

M.J. Prescott*
Mullard Central Technical Services

UDC 621. 397. 132

INTRODUCTION

Since the invention of the shadowmask, picture tube development has revolved almost exclusively around the delta-gun configuration. Refinement of this technology has resulted in extremely high quality colour reproduction which has fully justified the effort expended in its perfection. In recent years, however, several manufacturers have been investigating the possibilities of simplifying the conventional receiver. In particular, a great deal of research has been carried out on picture tubes incorporating in-line gun arrays. The main advantage offered by such a gun configuration compared with the conventional delta-gun array is that dynamic convergence corrections can at least be simplified, and at best, eliminated completely.

The 20AX system adopted by Mullard and introduced early in 1974, is the first inherently self-converging 110° colour television system capable of use with screen sizes up to 26in. It incorporates a horizontal-in-line gun array with a specially designed saddle-wound deflection yoke. The complex dynamic convergence correction circuits required by delta-gun receivers are eliminated. The only dynamic corrections required in 20AX are those to compensate for small residual manufacturing tolerances. These are few, and relatively straight-forward. In fact, only 7 simple dynamic corrections expending virtually no energy are required in a 20AX receiver compared with the 15 to 18 intricate energy-consuming corrections necessary in a comparable delta-gun set.

Colour selection is achieved by means of a vertically slotted shadowmask, the phosphors being deposited on the screen in vertical stripes. The tube has a standard 36·5mm neck, but because of modifications to the gun made possible by the elimination of pole pieces required for dynamic convergence corrections, the neck length is reduced by 20mm compared with its delta-gun equivalent.

This article describes briefly the theory behind 20AX, and gives details of the picture tube and deflection coil assembly.

CONVERGENCE AND DEFLECTION

In any colour television picture tube, the three electron beams are deflected by a common deflection field. This field not only deflects the beams but to some extent defocuses them, hence giving rise to convergence errors. The theory behind convergence errors caused by deflection fields has been covered in detail in a previous article (Ref. 1). For completeness, however, a simplified description of the theory is given here.

Consider a conical pencil of beams which, in the absence of a deflecting field, converges at the centre of the screen (see Fig. 1). From the behaviour of such a beam pencil in a deflection field, conclusions can be drawn about the behaviour of the three beams in a delta-gun picture tube.

---

*This article is based heavily on material from P.G.J. Barten of Philips Picture Tube Development Laboratory and J.Kaashoek of the Philips Radio and Television Component Design Laboratory, with comments by A. Ciuciura and J. Lammers of the Mullard Central Application Laboratory.

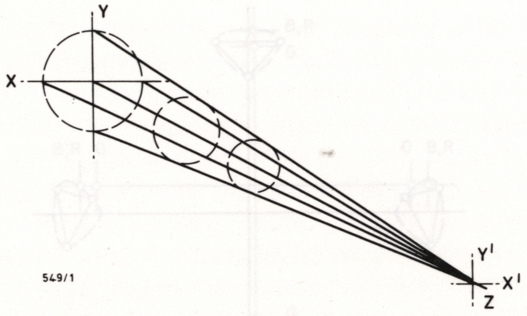

Fig. 1 — Conical pencil of beams originating in the deflection plane xy, and statically converged on the centre of the screen x'y'

Misconvergence

The main characteristics of a deflection field that determine its convergence properties are curvature of the image field, astigmatism, and coma.

Curvature of the image field results in the radius of curvature of the surface swept by the convergence point of the beam pencil being less than that of the screen (see Fig. 2). On a flat screen, the image of the beam pencil is circular. Considering the three beams for a delta-gun as elements of a beam pencil, it is seen in Fig. 3 that the convergence point on a flat screen forms an equilateral triangle.

The second characteristic, astigmatism, causes the convergence point of the beam pencil to separate into two focal lines, one parallel to, and one perpendicular to, the direction of deflection. One of these focal lines lies in front of the original convergence point, and the other behind it. The combined result of astigmatism and curvature of field on the three beams of a delta-gun tube is shown in Fig. 4. The image spots now form isosceles triangles, instead of the equilateral triangles resulting from curvature of field only. Fig. 5 shows how curvature

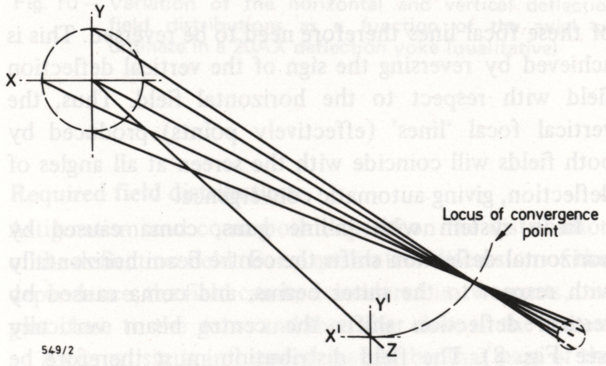

Fig. 2 — Deflected beam pencil. Locus of convergence point lies inside the plane of the screen; the image of the beam pencil on the screen is circular

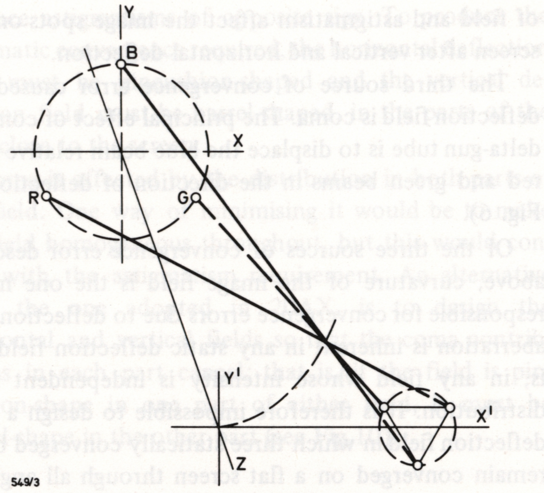

Fig. 3 — Convergence errors in a delta-gun tube caused by curvature of the image field

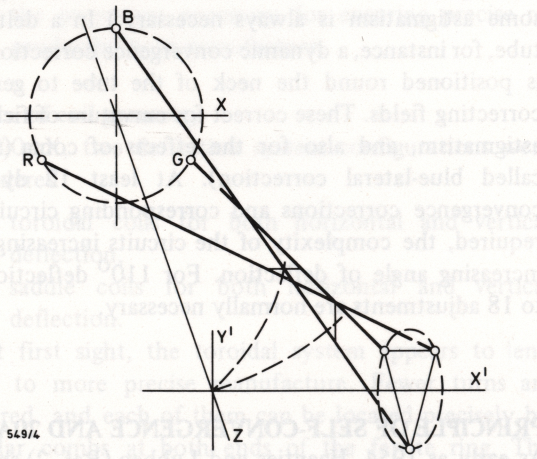

Fig. 4 — Convergence errors in a delta-gun tube caused by the combined effects of curvature of the image field and astigmatism

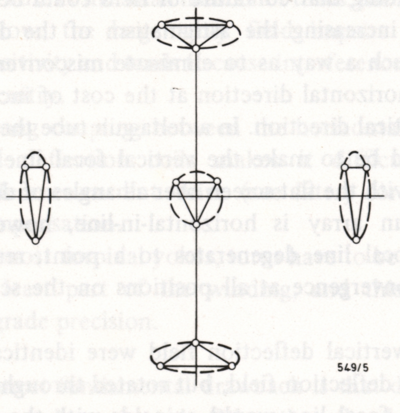

Fig. 5 — Convergence errors after vertical and horizontal deflection

of field and astigmatism affect the image spots on a flat screen after vertical and horizontal deflection.

The third source of convergence error caused by a deflection field is coma. The principal effect of coma in a delta-gun tube is to displace the blue beam relative to the red and green beams in the direction of deflection (see Fig. 6).

Of the three sources of convergence error described above, curvature of the image field is the one mainly responsible for convergence errors due to deflection. This aberration is inherent in any static deflection field; that is, in any field whose intensity is independent of its distribution. It is therefore impossible to design a static deflection field in which three statically converged beams remain converged on a flat screen through all angles of deflection. In practice, in a delta-gun tube, it is necessary to provide some means for varying the angles of the three beams according to the angle of deflection. The relative amplitudes of the required corrections depend on how much astigmatism there is in the horizontal and vertical deflection fields. (In fact, to obtain optimum convergence over the whole screen in a 110° system, some astigmatism is always necessary.) In a delta-gun tube, for instance, a dynamic convergence correction unit is positioned round the neck of the tube to generate correcting fields. These correct for curvature of field and astigmatism, and also for the effects of coma (the so-called blue-lateral correction). At least 12 dynamic convergence corrections and corresponding circuits are required, the complexity of the circuits increasing with increasing angle of deflection. For 110° deflection, 15 to 18 adjustments are normally necessary.

PRINCIPLE OF SELF-CONVERGENCE AND 20AX

As early as 1954, Haantjes and Lubben (Ref. 2) showed that it would be possible to eliminate convergence errors by adopting an in-line gun array in conjunction with a specially designed deflection assembly.

Their solution to the convergence problem was based on the finding that curvature of field could be compensated by increasing the astigmatism of the deflection field in such a way as to eliminate misconvergence in, say, the horizontal direction at the cost of increasing it in the vertical direction. In a delta-gun tube the effect of this would be to make the vertical focal line in Fig. 4 coincide with the flat screen over all angles of deflection. If the gun array is horizontal-in-line, however, this vertical focal line degenerates to a point, resulting in perfect convergence at all positions on the screen (see Fig. 7).

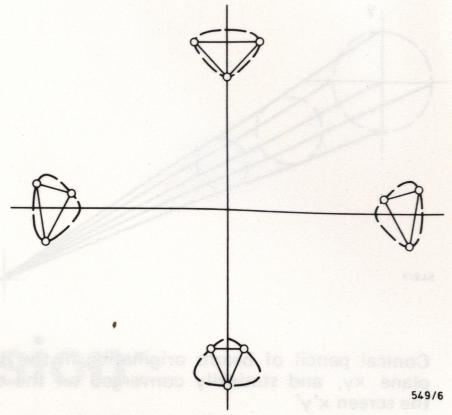

Fig. 6 — Distortion of the spot images caused by coma

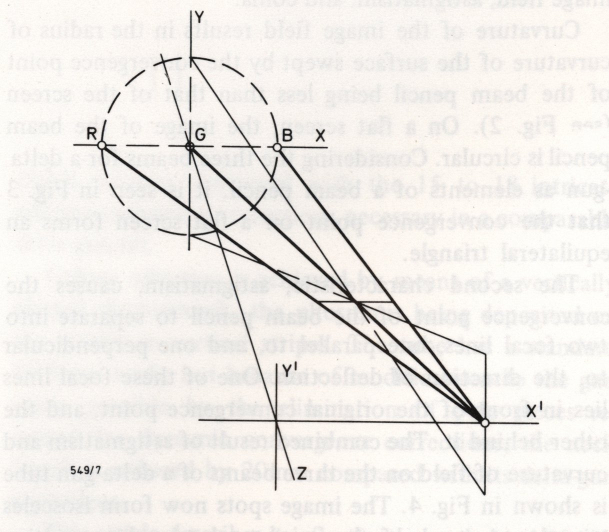

Fig. 7 — Automatic convergence in an in-line-gun tube produced by enhanced astigmatism of the deflection field

If the vertical deflection field were identical to the horizontal deflection field, but rotated through 90°, the horizontal focal line would coincide with the screen at all points, not the vertical one as required. The positions of these focal lines therefore need to be reversed. This is achieved by reversing the sign of the vertical deflection field with respect to the horizontal field. Thus, the vertical focal 'lines' (effectively points) produced by both fields will coincide with the screen at all angles of deflection, giving automatic convergence.

In a system with in-line guns, coma caused by horizontal deflection shifts the centre beam horizontally with respect to the outer beams, and coma caused by vertical deflection shifts the centre beam vertically (see Fig. 8). The field distribution must therefore be arranged in such a way as to virtually eliminate the coma errors shown in Fig. 8. This has been achieved in the 20AX system.

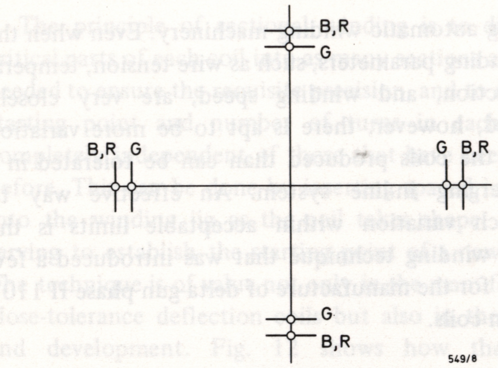

Fig. 8 — Convergence errors in an in-line-gun tube caused by coma

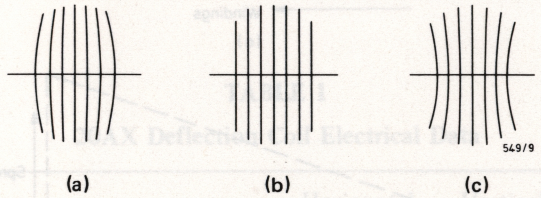

(a) (b) (c)

Fig. 9 — Three types of field distribution: (a) barrel (b) homogeneous (c) pincushion. The field distributions shown in (a) and (c) produce astigmatisms of opposite sign

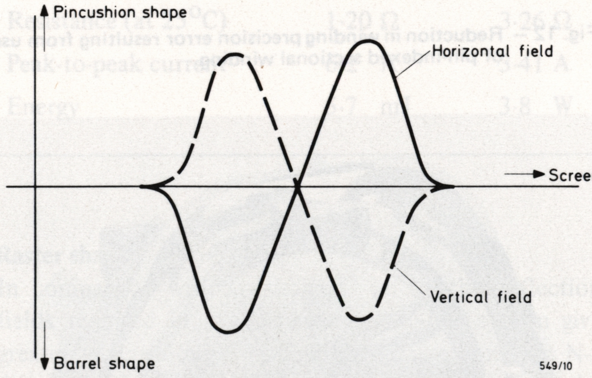

Fig. 10 — Variation of the horizontal and vertical deflection field distributions as a function of the axial coordinate in a 20AX deflection yoke (qualitative)

Required field distribution

Astigmatism and coma both depend on the distribution of the deflection field. For a qualitative discussion of this dependence, the field can be considered in two parts, one part close to the guns, and the other close to the screen.

Astigmatism is influenced mainly by that part of the field close to the screen. If the field distribution is homogeneous (see Fig. 9), astigmatism is approximately zero. Barrel-type distribution and pincushion-type distribution produce astigmatisms of opposite sign. To produce the automatic convergence required, the horizontal deflection field must be pincushion-shaped and the vertical deflection field must be barrel-shaped, in the parts of the field close to the screen.

Coma is affected by the distribution in both parts of the field. One way of minimising it would be to make the field homogeneous throughout, but this would conflict with the astigmatism requirement. An alternative way, the one adopted in 20AX, is to design the horizontal and vertical fields so that the coma contributions in each part cancel; that is, if the field is pincushion-shape in one part of either field, it must be barrel-shape in the other part (see Fig.10).

COIL DESIGN

The main aspects of coil design that must be considered are:

1) the shape of the coil to give the required field distribution;
2) the provisions necessary for ensuring precise reproducibility in manufacture.

Choice of coil geometry

For 20AX, two deflection system configurations were considered:

1) toroidal coils for both horizontal and vertical deflection,
2) saddle coils for both horizontal and vertical deflection.

At first sight, the toroidal system appears to lend itself to more precise manufacture. Fewer turns are required, and each of them can be located precisely by annular combs at both ends of the ferrite ring. The material content is low and manufacture can be easily mechanised.

However, for all its apparent simplicity, the toroidal yoke does have important limitations.

1) Because of the small number of turns, the impedance is low; the large stray field impairs deflection sensitivity and tends to cause interference in nearby circuitry.
2) Strong coupling between the horizontal and vertical deflection coils makes it difficult to use difference-current drive (see later) for tolerance compensation.
3) In most toroidal yokes, turns have to be layered in at least part of the winding, and this tends to degrade precision.

But the most fundamental drawback is that design freedom is severely restricted. Other than the shape of the core, the only design parameter is the angular positioning of the turns, and since no position should be assigned to more than one turn, the horizontal and vertical deflection coils cannot be designed independently of each other.

Studies led to the conclusion that these limitations make the toroidal yoke impracticable for generating the coma-free fields required in 20AX. Additional design parameters would be necessary, thereby adding to the complexity of the yoke and increasing its final cost. A saddle-type yoke assembly was therefore adopted for 20AX.

The relationship between field distribution and saddle coil shape can be best illustrated by considering a constant diameter coil comprising two symmetrical, single-turn windings (see Fig. 11). Angle α is an important design parameter (Ref. 1). If $\alpha \simeq 120^{\circ}$, the field close to the axis z is homogeneous; if $\alpha > 120^{\circ}$, the field is pincushion-shape, and if $\alpha < 120^{\circ}$, the field is barrel-shaped.

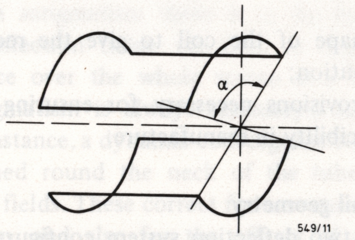

Fig. 11 – Schematic representation of a symmetrical pair of single-turn deflection coils; angle α is the angle subtended by the coils

To produce the field distribution required for the 20AX self-converging system, angle α must vary along the length of the deflection coil. For the horizontal deflection coil, α must increase from about 90° at the gun end to about 150° at the screen end to avoid coma errors. For the vertical deflection coil, exactly the opposite variation is required; that is, from 150° at the gun end to 90° at the screen end.

This simple description considers only the lower order terms in the equations describing the field produced by a symmetrical pair of single-turn windings. However, undesirable effects due to large, higher-order terms can be minimised by adding more turns to each winding and carefully defining their positions. The final coil design for 20AX employs a relatively large number of turns accurately distributed around the inside of the ferrite core. The distribution varies along each coil in such a way as to provide the required astigmatism and absence of coma necessary to achieve optimum convergence over the whole screen.

Coil manufacture

The manufacture of such coils in large quantities and to the required accuracy presents certain difficulties. Coils of complex shape can be wound on specially designed jigs, using automatic winding machinery. Even when the usual winding parameters, such as wire tension, temperature, friction, and winding speed, are very closely controlled, however, there is apt to be more variation between the coils produced than can be tolerated in a self-converging in-line system. An effective way to bring such variation within acceptable limits is the sectional winding technique that was introduced a few years ago for the manufacture of delta-gun phase II 110° deflection coils.

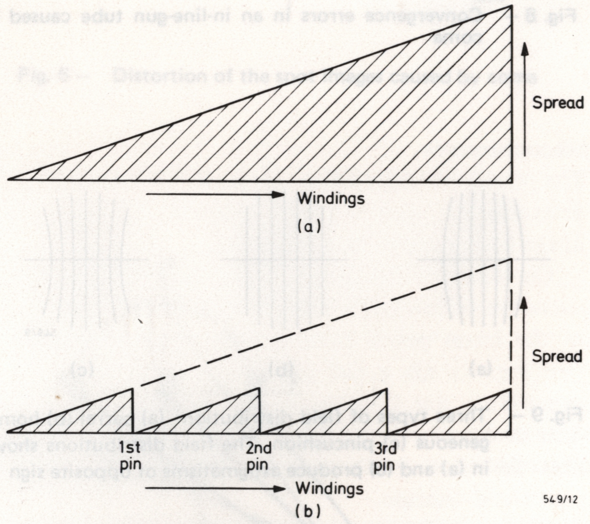

Fig. 12 – Reduction in winding precision error resulting from use of pin-indexed sectional winding

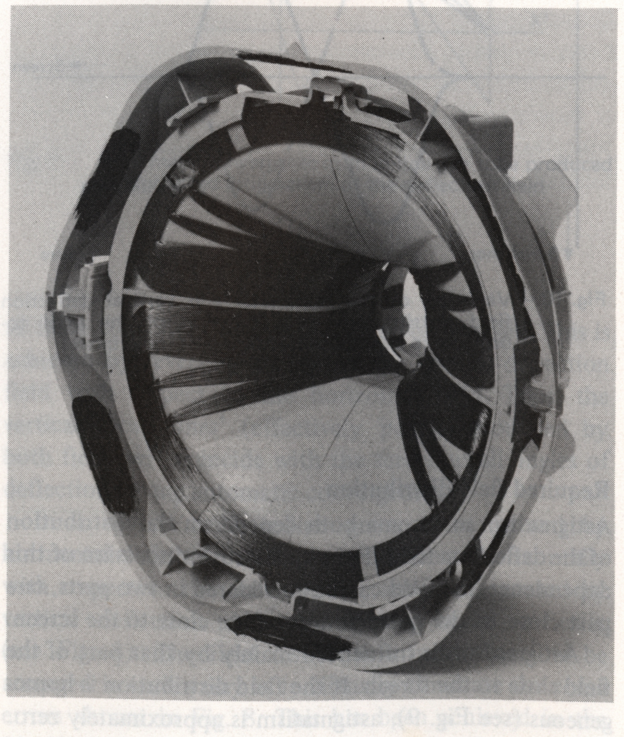

Fig. 13 – Horizontal deflection coils mounted in 20AX yoke

The principle of sectional winding is to divide the critical parts of each coil into as many sections as may be needed to ensure the requisite precision, and to make the starting point and number of turns in each section completely independent of those that have been wound before. This can be done by inserting spaced index pins into the winding jig as the coil takes shape, each pin serving to establish the starting point of a new section. The technique is of value not only in the manufacture of close-tolerance deflection coils but also in their design and development. Fig. 12 shows how the overall precision error is reduced by sectional pin indexing. Table 1 gives the electrical specifications for the horizontal and vertical deflection coils. In Fig. 13, the horizontal deflection coils are shown mounted in the deflection yoke. A cutaway view of the deflection assembly is shown in Fig. 19. More details of deflection coil design and manufacture are given in Ref. 1.

TABLE 1

20AX Deflection Coil Electrical Data

	Horizontal deflection coil	Vertical deflection coil
Inductance	1·18 mH	35 mH
Resistance (at 25°C)	1·20 Ω	3·26 Ω
Peak-to-peak current	6·2 A	3·41 A
Energy	5·7 mJ	3·8 W

Raster shape

In comparison with a delta-gun system, the deflection fields required in a self-converging in-line system give greater pincushion E-W raster distortion but less N-S distortion. Because of the sign of the astigmatism, the N-S distortion is barrel-shaped. N-S raster distortion can be decreased still further by treating the shape of the ferrite ring as an additional design parameter. In the 20AX deflection unit, shaped cut-outs (Fig. 14) at the gun end of the ferrite ring are positioned so that they affect only the vertical deflection field, giving a N-S raster shape which is fully acceptable without further correction. The E-W raster distortion of 13% is corrected by means of conventional deflection current modulating circuitry.

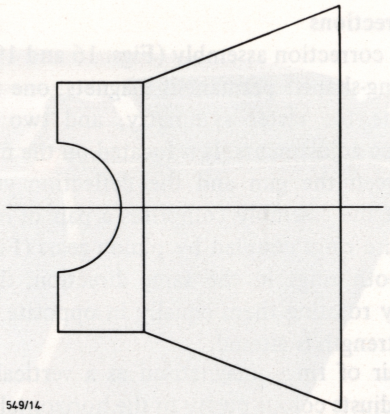

Fig. 14 – Schematic outline of ferrite core (side elevation) showing one of the field shaper cut-outs

Mechanical assembly

In addition to the measures taken to achieve the highest possible precision in the manufacture of the deflection coils, special attention is also paid to their assembly. The coils are mounted in a split plastic shell which incorporates moulded-in locating pieces for each winding. This secures them in the correct position relative to the ferrite ring, regardless of small variations in turn distribution. The coils and ferrite ring are mounted as an adjustable unit in a housing (Figs. 15 and 19) that clamps to the neck of the tube and engages a centring ridge moulded into the cone. Only two adjustments are provided: a ± 7° rotation for raster alignment, and a 6mm axial shift for colour purity. Clamps on the housing lock the unit in the desired position. The axial movement is provided by an adjustable ring at the back of the housing, the coil moving in a helical slot in the circumference.

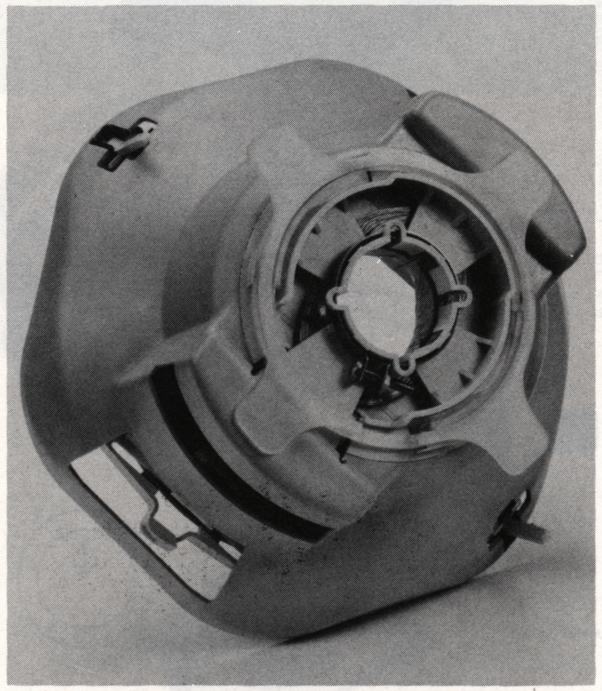

Fig. 15 – 20AX deflection yoke housing

Static corrections

The static correction assembly (Figs. 16 and 19) consists of four ring-shaped permanent magnets; one for colour purity, one for raster symmetry, and two for static convergence adjustments. It is located on the neck of the tube between the gun and the deflection yoke. Each element of the assembly comprises a pair of magnetised plasto-ferrite rings coupled by pinion gears (Fig. 17). By rotating both rings in the same direction, the field is rotated; by rotating them equally in opposite directions the field strength is altered.

One pair of rings, magnetised as a vertical two-pole magnet, adjusts colour purity in the horizontal direction.

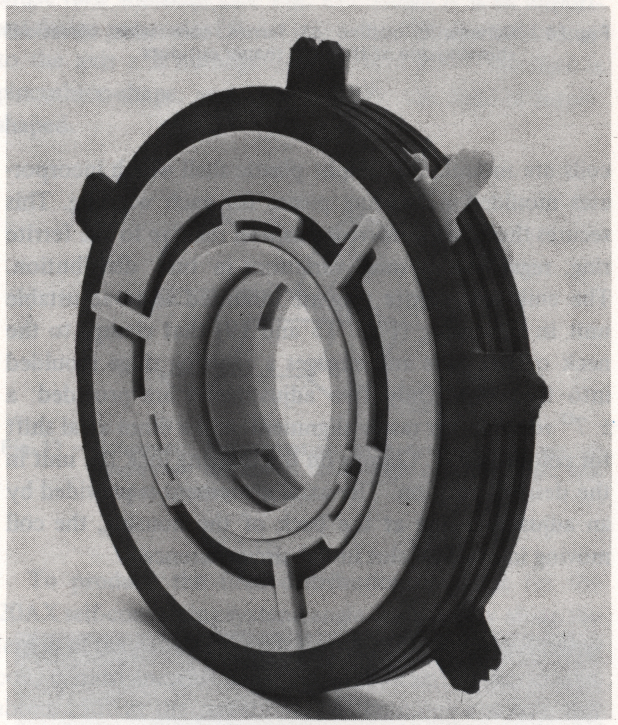

Fig. 16 — Static correction unit

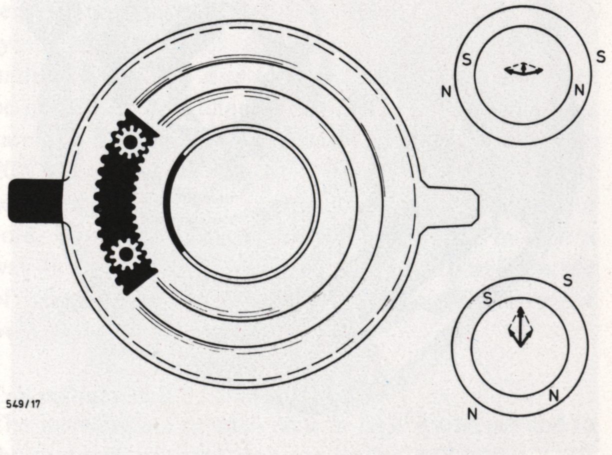

Fig. 17 — Pair of plasto-ferrite magnet rings as used in static correction assembly, showing coupling pinions

Another pair, magnetised as a horizontal two-pole magnet, corrects any vertical misalignment there may be between the beams and the axis of the tube-yoke system. Owing to the strong astigmatism of the horizontal deflection field, such misalignment would otherwise cause curvature of the horizontal axis of the raster. Two pairs of rings allow for static convergence correction, one magnetised as a four-pole magnet, and the other as a six-pole magnet. Adjustment of the four-pole pair pre-deflects the two outer beams equally in opposite directions, and adjustment of the six-pole pair pre-deflects them equally in the same direction, making it possible to bring all three beam spots into coincidence on the screen.

The complete multi-pole static correction assembly fits flush with the rear of the deflection coil housing on the neck of the tube (see Fig. 19). It is located by a key and slot in the housing, and is locked by a finger-operated clamp on the multi-pole unit.

20AX PICTURE TUBE

Externally there is little to distinguish a 20AX picture tube (Fig. 18) from a comparable delta-gun 110° type apart from the shorter neck and the deflection yoke centring ridge on the cone. Internally, however, there are fundamental differences. A cutaway view of a 20AX picture tube, deflection yoke, and static correction assembly is shown in Fig. 19.

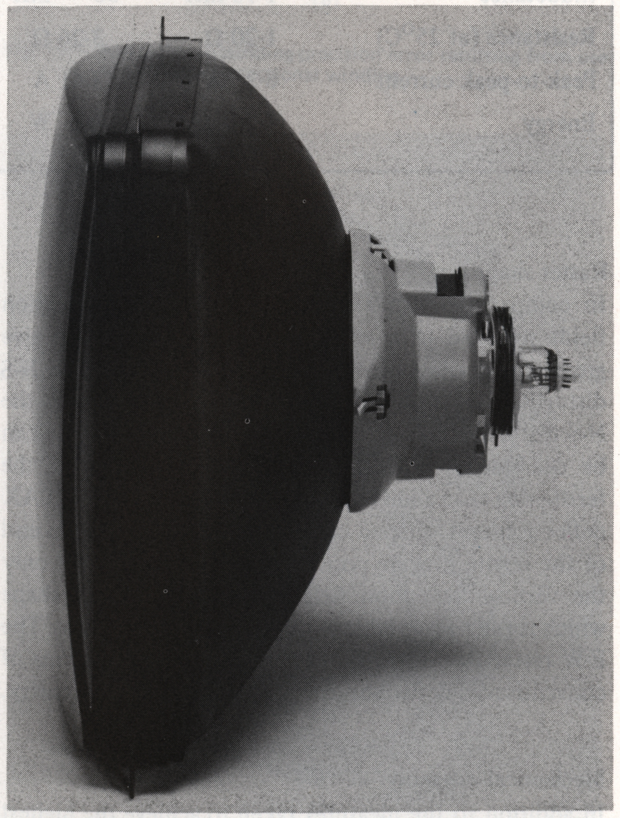

Fig. 18 — 20AX picture tube and deflection yoke.

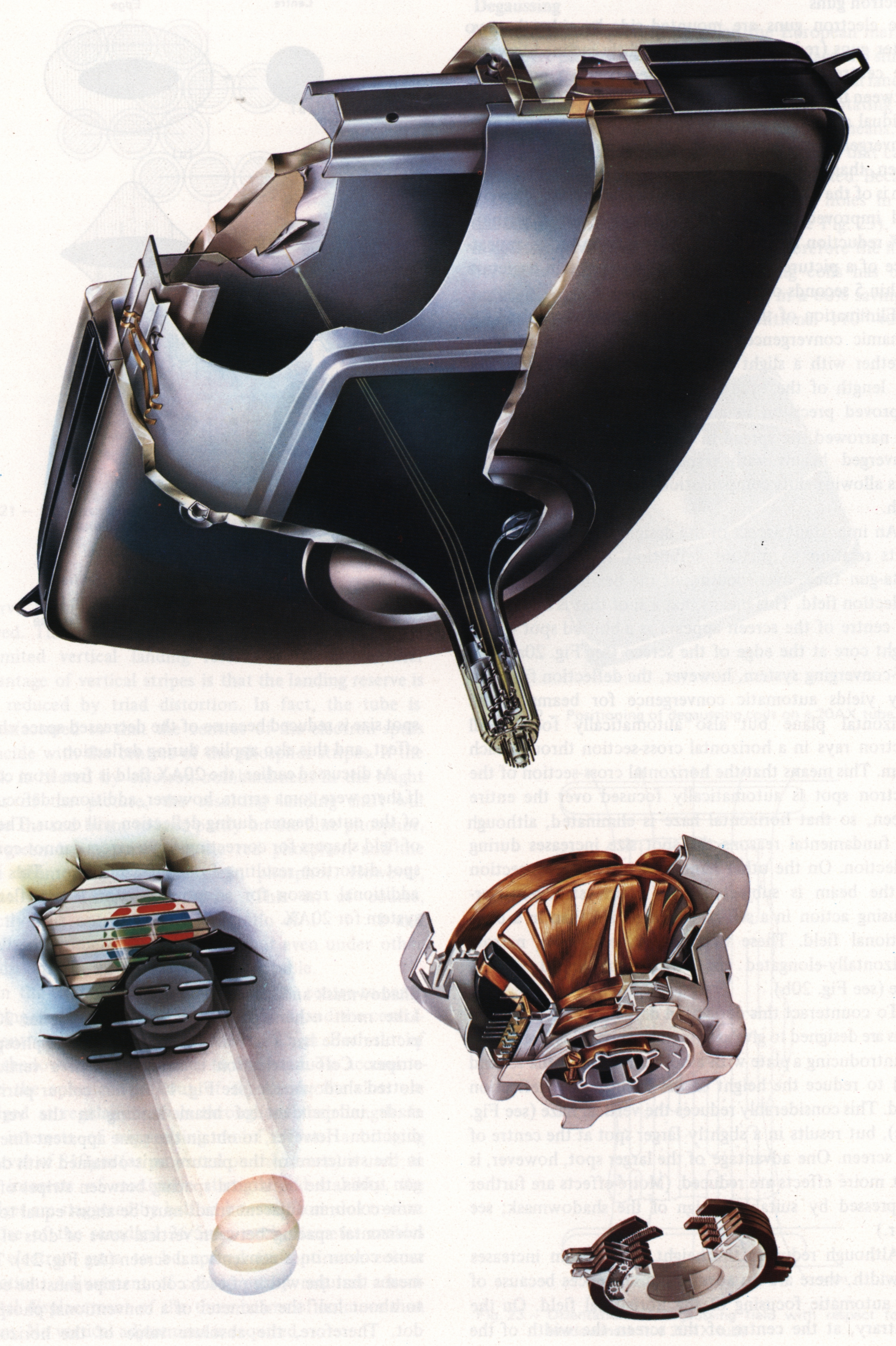

Fig. 19 — Cutaway view of 20AX picture tube, deflection yoke and static correction assembly

Electron guns

The electron guns are mounted side by side, the two outer guns (red and blue) being slightly inclined towards the centre gun (green). The green beam is positioned between the other two to reduce the effect of small residual convergence errors. (The eye is more sensitive to convergence errors between red and green, or blue and green, than between red and blue.) The cathode of each gun is of the Quick-vision type with low thermal capacity and improved heater-to-cathode heat transfer, giving a 70% reduction in the time from switch-on to the appearance of a picture. It is thus possible to obtain a picture within 5 seconds of switch-on.

Elimination of the pole shoes (normally required for dynamic convergence) at the muzzle end of the gun, together with a slight reduction in gun length, enables the length of the tube neck to be reduced by 20mm. Improved precision in gun manufacture and assembly has narrowed the spread in the position of the statically converged beams with respect to the screen centre, thus allowing shift compensation circuits to be dispensed with.

An important aspect of the design of the electron gun is its relation to picture definition. In a conventional delta-gun tube, over-focusing of the beam occurs in the deflection field. This means that a spot that is in focus at the centre of the screen appears as a blurred spot with a bright core at the edge of the screen (see Fig. 20a). In a self-converging system, however, the deflection field not only yields automatic convergence for beams in the horizontal plane but also automatically focuses all electron rays in a horizontal cross-section through each beam. This means that the horizontal cross-section of the electron spot is automatically focused over the entire screen, so that horizontal haze is eliminated, although for fundamental reasons the spot size increases during deflection. On the other hand, the vertical cross-section of the beam is subjected to a much stronger over-focusing action in a self-converging field than in a conventional field. These two factors result in a narrow horizontally-elongated spot with pronounced vertical haze (see Fig. 20b).

To counteract this deflection defocusing, the electron guns are designed to give astigmatic beams. This is achieved by introducing a plate with a horizontal slit in the second grid to reduce the height of the beam in the deflection field. This considerably reduces the vertical haze (see Fig. 20c), but results in a slightly larger spot at the centre of the screen. One advantage of the larger spot, however, is that moiré effects are reduced. (Moiré effects are further suppressed by suitable design of the shadowmask; see later.)

Although reducing the height of the beam increases its width, there are no adverse consequences because of the automatic focusing of the horizontal field. On the contrary, at the centre of the screen the width of the spot size is reduced because of the decreased space charge effect, and this also applies during deflection.

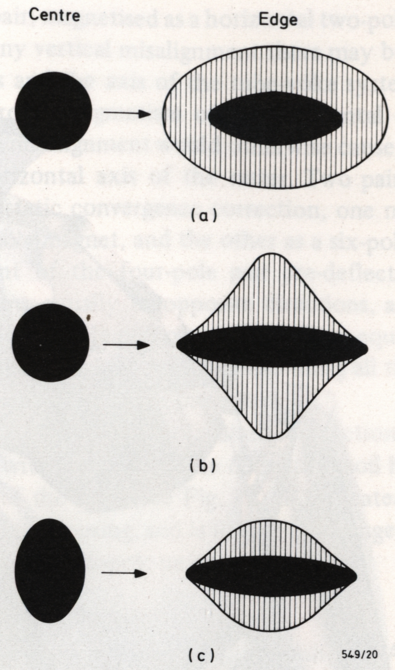

Fig. 20 — Defocusing of a round spot in:
(a) conventional deflection field
(b) self-converging deflection field
(c) reduction of defocusing by use of an astigmatic gun

As discussed earlier, the 20AX field is free from coma. If there were coma errors, however, additional defocusing of the outer beams during deflection will occur. The use of field shapers for correcting coma errors cannot correct spot distortion resulting from the same error. This is an additional reason for adopting a coma-free deflection system for 20AX.

Shadowmask and screen

Like most other tubes with in-line guns, the 20AX picture tube has a screen consisting of vertical phosphor stripes. Colour selection is achieved with a vertically slotted shadowmask (see Fig. 19). Thus colour purity is made independent of beam landing in the vertical direction. However, to obtain the same apparent fineness in the structure of the picture as is obtained with delta-gun tubes, the horizontal spacing between stripes of the same colour in adjacent triads must be about equal to the horizontal spacing between vertical rows of dots of the same colour on a conventional screen (see Fig. 21). This means that the width of each colour stripe must be equal to about half the diameter of a conventional phosphor dot. Therefore, the absolute value of the horizontal

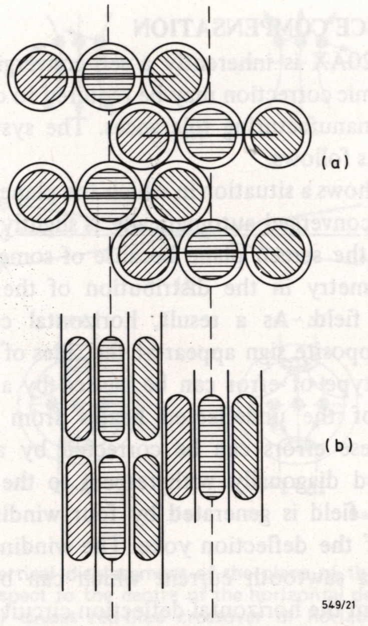

Fig. 21 — Dot-structure screen (a) compared with a stripe-structure screen (b) of equal fineness

reserve, assuming equal mask transmission, is about halved. This disadvantage must be weighed against the unlimited vertical landing reserve. However, another advantage of vertical stripes is that the landing reserve is not reduced by triad distortion. In fact, the tube is manufactured so that the centres of the electron spots coincide with the centres of the phosphor stripes. If the mask is heated by electron bombardment in the bright areas of the picture, the resulting landing shift will cause the red beam to land partly on the blue phosphor, the green beam partly on the red phosphor, and the blue beam partly on the green phosphor. However, white will still remain white. This is, of course, strictly true only for a current ratio of 1 : 1 : 1 and idealised geometrical conditions, but even under other conditions, the advantage is still noticeable.

In the 26in 20AX picture tube, the centre-to-centre spacing of the phosphor stripes is 265μm, and the centre-to-centre spacing of adjacent triads, 795μm. Each slot of the shadowmask corresponds to one triad. To accommodate the spherical contour of the mask, the slots are bridged at regular intervals throughout their length. In the interests of suppressing moiré effects, a bridging interval of 810μm (as projected on the screen) is used; in the interests of maximum strength and stability, the bridges are staggered by half an interval from slot to slot.

Use of the standard 36·5mm neck diameter enables the electron guns to be spaced for optimum colour selection. Adjustment of colour purity requires a horizontal displacement of the three beams of no more than 45μm. No vertical adjustment is required.

Degaussing

Like most 110° picture tubes on the European market, the 20AX picture tube uses an internal magnetic shield. Advantage has been taken of the unlimited vertical landing reserve inherent in the 20AX system by rotating the degaussing coils through 90° (Fig. 22). By this means, the vertical component of residual magnetic fields that cause horizontal landing errors is completely eliminated. Because the mask material is not interrupted by holes in the direction of the degaussing field lines (see Fig. 23), the magnetomotive force can be smaller. Therefore the number of ampere-turns in the degaussing coils has been reduced from 500 to 300, resulting in a 60% saving of copper wire compared with conventional 110° tubes.

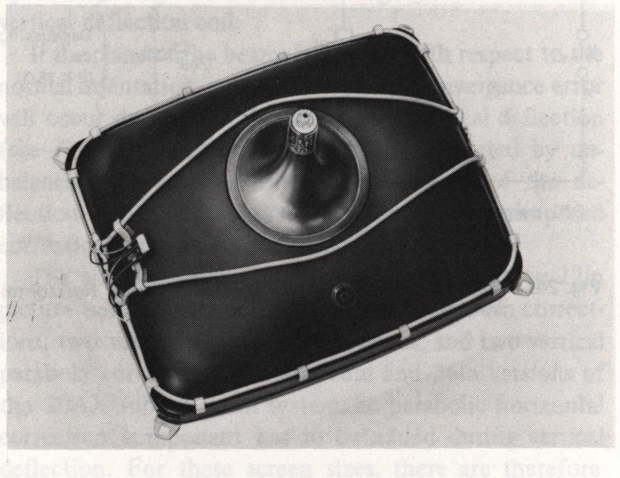

Fig. 22 — Positioning of degaussing coils on a 20AX tube.

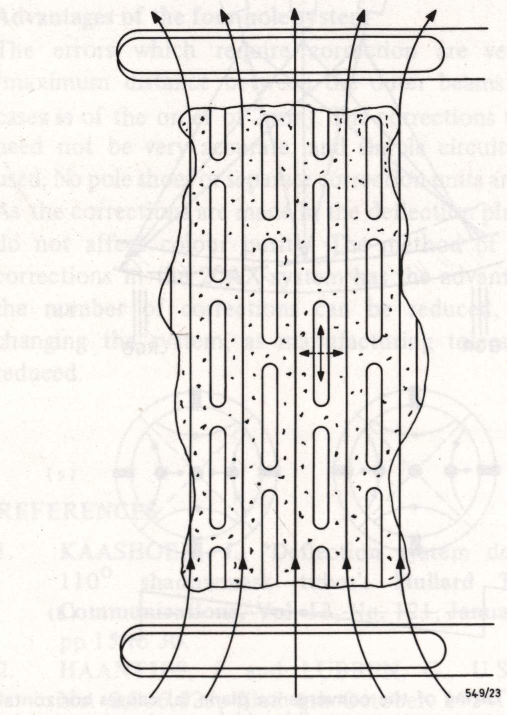

Fig. 23 — Orientation of degaussing field with respect to the shadowmask in a 20AX tube

To eliminate the risk of mis-landing caused by currents induced in the degaussing coils by the horizontal deflection field, the degaussing coils are short-circuited at horizontal deflection frequencies by a 0·1µF capacitor Except for this additional capacitor, the degaussing circuit (see Fig. 24) is the same as is used with a Phase II 110° picture tube.

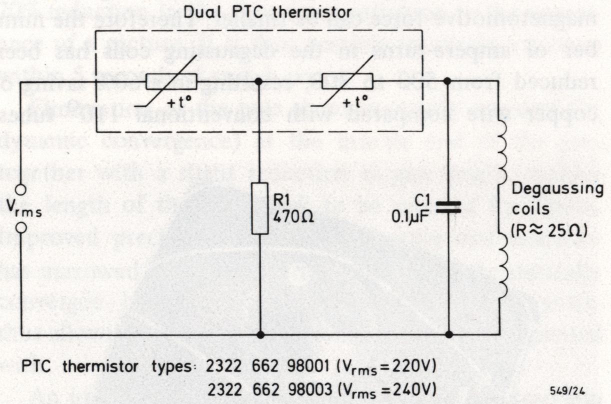
Dual PTC thermistor
+t°
+t°
R1
470Ω
C1
0.1µF
Degaussing coils
(R≈ 25Ω)
V_rms
PTC thermistor types 2322 662 98001 (V_rms = 220V)
2322 662 98003 (V_rms = 240V)
549/24

Fig. 24 – Recommended degaussing circuit with horizontal-frequency interference suppression capacitor

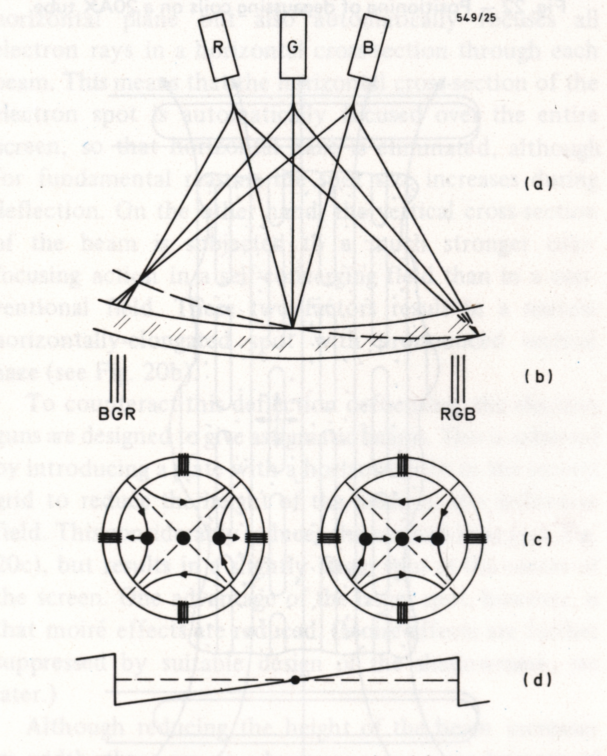

Fig. 25 – Tilting of the convergence plane (a) causes horizontal convergence errors (b) which can be corrected by four-pole windings (c) driven by a sawtooth current of line frequency (d)

TOLERANCE COMPENSATION

Although 20AX is inherently a self-converging system, some dynamic correction may be required to compensate for small manufacturing tolerances. The system can be explained as follows.

Fig 25 shows a situation in which the plane where the beams are converged automatically is slightly tilted with respect to the screen plane because of some small left-right asymmetry in the distribution of the horizontal deflection field. As a result, horizontal convergence errors of opposite sign appear at the sides of the screen. The same type of error can be caused by a horizontal deviation of the undeflected beams from the screen centre. These errors can be corrected by a four-pole field aligned diagonally with respect to the deflection fields. This field is generated by four windings around the core of the deflection yoke. The windings must be driven by a sawtooth current which can be obtained directly from the horizontal deflection circuit.

In the same way, top-to-bottom asymmetry of the vertical deflection field, or a vertical deviation of the undeflected beams from the screen centre, causes horizontal convergence errors at the top and bottom of the screen. These errors can be corrected by passing sawtooth currents at vertical deflection frequency through the four-pole windings.

Horizontal displacement of the electron beams with respect to the deflection coil centre is not normally detrimental, because the system automatically converges all the beams which lie in a horizontal plane through the coil axis. However, vertical displacement of the plane of the beams with respect to the centre of the deflection field causes horizontal convergence errors of sawtooth character during vertical deflection (see Fig. 26). These errors can also be corrected by passing currents at vertical deflection frequency through the four-pole windings. At the same time, however, vertical convergence errors will appear during horizontal deflection and will cause crossover of the horizontal red and blue lines (see Fig. 27). The same type of error can also be caused by top-to-bottom asymmetry of the horizontal deflection field.

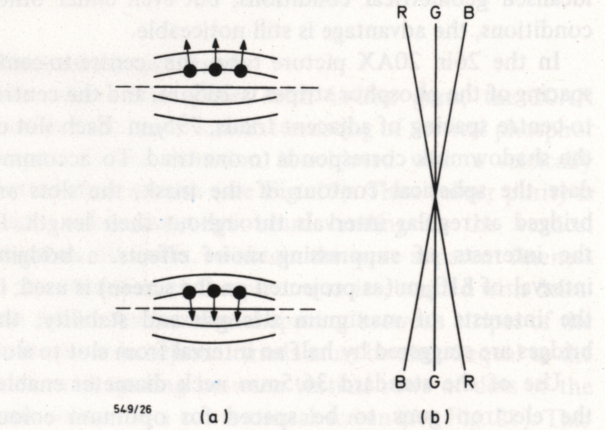

Fig. 26 – Vertical displacement of the plane of the beams with respect to the centre of the vertical deflection (a) causes red-blue crossover of vertical lines (b)

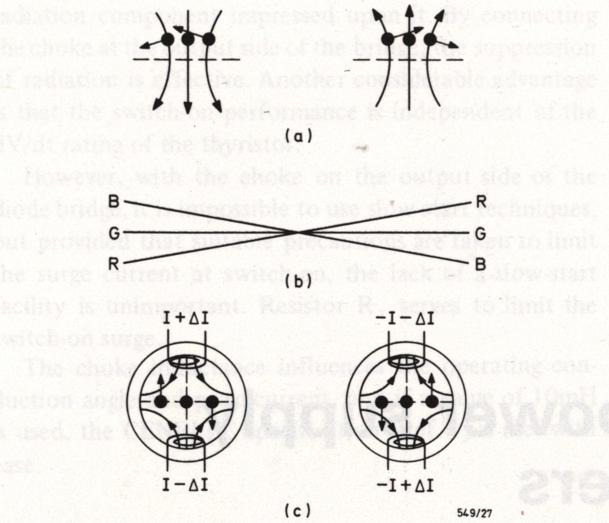

Fig. 27 – Vertical displacement of the plane of the beams with respect to the centre of the horizontal deflection field (a) causes red-blue crossover of horizontal lines (b) which can be corrected by unbalancing the horizontal deflection coil halves (c)

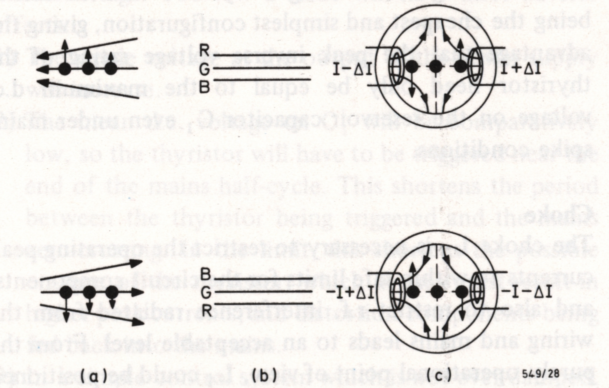

Fig. 28 – Left-right asymmetry of the vertical deflection field (a) causes vertical misconvergence at top and bottom of the picture (b) which can be corrected by unbalancing the vertical deflection coil halves (c)

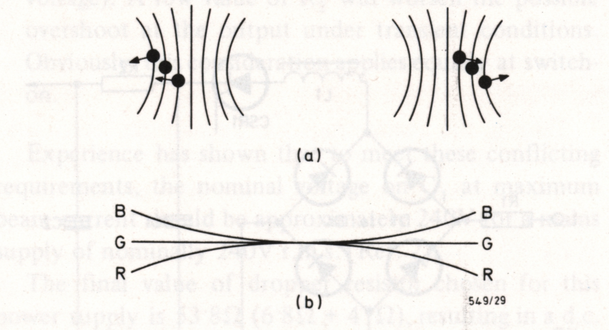

Fig. 29 – Rotation of the electron gun (a) causes vertical convergence errors of parabolic character (b)

These errors can be corrected by a four-pole field which is aligned orthogonally with respect to the deflection fields. This type of four-pole field can be generated by unbalancing the current through the halves of the horizontal deflection coil. Similarly, left-to-right asymmetry of the vertical deflection field, or horizontal deviation of the undeflected beams from the screen centre, causes vertical convergence errors during vertical deflection (see Fig. 28). These errors can be corrected by unbalancing the current through the halves of the vertical deflection coil.

If the plane of the beams is rotated with respect to the normal orientation, a parabolic vertical convergence error will occur during both horizontal and vertical deflection (see Fig. 29). This error can also be corrected by unbalancing the current through the halves of the deflection coil. In this case, however, the superimposed correction current must be parabolic.

The six corrections so far mentioned apply to 22in picture tubes; they are two horizontal sawtooth corrections, two vertical sawtooth corrections, and two vertical parabola corrections. For the 18in and 26in versions of the 20AX tube, a small systematic parabolic horizontal correction component has to be added during vertical deflection. For these screen sizes, there are therefore seven corrections.

Advantages of the four-pole system

The errors which require correction are very small (maximum distance between the outer beams in most cases is of the order of 2mm). The corrections therefore need not be very accurate, and simple circuits can be used. No pole shoes or separate correction units are needed As the corrections are made in the deflection plane, they do not affect colour purity. The method of applying corrections in the 20AX system has the advantage that the number of corrections can be reduced, without changing the system, as manufacturing tolerances are reduced.

REFERENCES

1. KAASHOEK, J., 'Deflection system design for 110° shadowmask tubes', **Mullard Technical Communications**, Vol. 13, No. 121, January 1974, pp 15 to 30.
2. HAANTJES, J. and LUBBEN, G., U.S. Patent No. 2,866,125, filed 6th October, 1954. See also 'Errors of magnetic deflection II', **Philips Research Reports**, Vol. 14, 1959, pp 65 to 97.

Full-wave thyristor power supply for television receivers

R.E.F. BUGG
Mullard Central Application Laboratory

UDC 621.311.62 [621.382.333.4] 621.397.132

A full-wave thyristor power supply for colour television receivers requiring an h.t. supply of 165V at 1A is described. The circuit is designed to give minimal harmonic and d.c. feedback into the mains. A low-temperature-coefficient crowbar overvoltage protection circuit is also described.

INTRODUCTION

In designing the power supply described in this article, efforts have been made to comply with the desire of the United Kingdom Central Electricity Generating Board to limit the levels of harmonic and d.c. feedback into the mains. As a result of this and of other considerations concerned with the spreads and tolerances of the thyristor and the trigger element, a full-wave circuit has been developed which is suitable for any receiver requiring an h.t. supply of 165V at 1A. Such a circuit offers several advantages over the currently-used half-wave designs.

1) No d.c. component of current is drawn from the mains.
2) The peak current drawn from the mains is substantially lower, and hence harmonic distortion is reduced.
3) Even-order harmonic distortion is eliminated.
4) Smoothing capacitors are reduced in size.
5) The peak inverse voltage requirement of the thyristor is reduced.

The main disadvantage is that the chassis of the receiver is 'live'.

CHOICE OF MAJOR COMPONENTS

The major components of the power supply are shown in Fig. 1. It is worthwhile considering the configuration and values used for these components.

Configuration

A diode bridge and a single thyristor were chosen as being the cheapest and simplest configuration, giving the advantage that the peak inverse voltage rating of the thyristor need only be equal to the maximum d.c. voltage on the reservoir capacitor C_1 even under mains spike conditions.

Choke

The choke L_1 is necessary to restrict the operating peak currents to within safe limits for the circuit components, and also to restrict r.f. interference radiated from the wiring and mains leads to an acceptable level. From the purely operational point of view, L_1 could be positioned either at the input or the output side of the diode bridge. However, if the choke were connected at the input side of the bridge, the radiation voltage components developed across the choke would appear between chassis and live, and between chassis and neutral, on alternate half-cycles; that is, the chassis would have a substantial radiation component impressed upon it. By connecting the choke at the output side of the bridge, the suppression of radiation is effective. Another considerable advantage is that the switch-on performance is independent of the dV/dt rating of the thyristor.

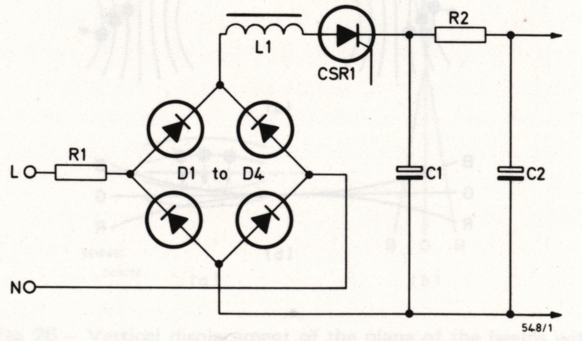

Fig. 1 — Major components of power supply

However, with the choke on the output side of the diode bridge, it is impossible to use slow-start techniques, but provided that suitable precautions are taken to limit the surge current at switch-on, the lack of a slow-start facility is unimportant. Resistor R_1 serves to limit the switch-on surge.

The choke inductance influences the operating conduction angle and peak current, and if a value of 10mH is used, the CENELEC specification (Ref. 1) is met with ease.

Dropper resistor

The dropper resistor R_2 (Fig. 1) defines the ripple voltage at the output of the power supply and determines the d.c. voltage on C_1 at a given load current. Too high a value of R_2 will result in excessive dissipation, and ultimately insufficient output voltage at low values of mains voltage. Too low a value will have three adverse effects.

1) The ripple voltage at the output of the power supply will increase.
2) The mean d.c. voltage on C_1 will be comparatively low, so the thyristor will have to be triggered near the end of the mains half-cycle. This shortens the period between the thyristor being triggered and the mains zero-crossing. In the limit, this shortens the possible on-time of the thyristor, which in turn must result in higher peak currents, and distortion components being fed back into the mains.
3) In a simple control system which is not over-damped, there will always be an overshoot in the d.c. voltage on C_1 in response to a transient in the load current. If the normal operating voltage on C_1 is close to peak mains voltage, the overshoot on C_1, and thus the overshoot at the output, will be effectively limited (the voltage on C_1 cannot exceed peak mains voltage). A low value of R_2 will worsen the possible overshoot at the output under transient conditions. Obviously, this consideration applies equally at switch-on.

Experience has shown that to meet these conflicting requirements, the nominal voltage on C_1 at maximum beam current should be approximately 240V for a mains supply of nominally 240V r.m.s. (Ref. 2).

The final value of dropper resistor chosen for this power supply is 53·8Ω (6·8Ω + 47Ω), resulting in a d.c. voltage on C_1 of 219V at an output current of 1A. This component is the major cause of heat loss in the power supply: the overall efficiency of the circuit is about 70%.

Capacitors

The values of the reservoir and smoothing electrolytic capacitors C_1 and C_2 (Fig. 1) determine the amplitude of ripple voltage at the output of the power supply in the normal way. However, in a thyristor power supply, where the output voltage is much less than the peak mains voltage, the ratio of the capacitors is also important when the transient response of the system is considered. Consider, for example, the effect of a flashover in the picture tube. After flashover, the line timebase will draw a considerable overcurrent as the e.h.t. capacitance is recharged. The feedback loop in the power supply will attempt to maintain the output voltage constant by increasing the voltage on the reservoir capacitor C_1. As soon as the e.h.t. capacitance is recharged, the overcurrent will disappear, but C_1 will still be charged to a voltage higher than its normal operating voltage. If the overcurrent is considerably greater than the normal current capability of the power supply, the overvoltage on C_1 will be approximately peak mains voltage, independent of the characteristics of the control circuit. If the capacitors C_1 and C_2 are of equal value, this will result in a considerable overshoot at the output of the power supply as the total charge is effectively 'shared' between the two capacitors.

The optimum solution in this case appears to be that the nominal value of C_1 should be about half that of C_2, depending on the effective series input resistance. This, and ripple considerations, results in the nominal values of C_1 and C_2 being made 500 and 800µF respectively. (See Appendix 2 for a summary of the ratings of the high-voltage electrolytic capacitors.)

THYRISTOR TRIGGERING CONTROL CIRCUIT

The control circuit is essentially similar to that in the currently-used half-wave design which uses a BR100 diac. In both circuits, a voltage ramp is applied to a timing capacitor until the capacitor voltage exceeds a reference voltage. When this occurs, the timing capacitor is discharged through a coupling capacitor into the thyristor gate. Feedback is effected by controlling the slope of the ramp by means of a transistor with mains voltage feed-forward and output voltage feedback applied to its base.

Desirable features

Experience with the half-wave circuit has shown that several features in a thyristor power supply control circuit are important.

1) The reference potential for determining the trigger point of the trigger element should have a well-defined voltage and a well-defined temperature coefficient.
2) The state of charge of the timing capacitor at the end of a mains half-cycle (that is, at the beginning of the next) should be independent of events during that half-cycle. That is, there should only be a 'memory'

effect from half-cycle to half-cycle in the main electrolytic capacitors C_1 and C_2 of Fig. 1, not in the control circuit.

3) As a result of (1), it was decided to use a voltage reference diode to determine the reference potential for the trigger element, and to use a silicon controlled switch (BR101) as the trigger element itself. If the SCS is to work effectively, its turn-off must be well defined and not a function, for example, of its holding current.

Circuit description

Fig. 2 shows the power supply circuit diagram. The timing ramp, generated by R_8 and C_7, is applied to the anode of the silicon controlled switch, type BR101. When this ramp voltage exceeds the reference potential set by D_8, the SCS is turned on via R_9 in the anode gate. Capacitor C_7 is then discharged into R_{11}, the resultant pulse being coupled via C_{10} into the thyristor gate. (The thyristor ratings are given in Appendix 2.)

The slope of the ramp is controlled by transistor TR_2. This has a proportion of the reference voltage of D_8 applied to its emitter via resistors R_{13} and R_{14}, which also define the gain of the stage. Output voltage feedback and mains feedforward are applied to the base of TR_2, via R_{19} and R_7. The potentiometer R_{15} enables adjustment of the h.t. voltage. It is positioned so that its drift with life has the minimum effect on the output voltage of the supply.

The resistors R_4 and R_5 perform two functions. While the mains voltage is greater than about 100V, C_{13} is being charged via D_6, and during the mains zero-crossing, the base of the emitter follower TR_1 is earthed via D_5.

Turning TR_1 on during the mains zero-crossing has three important effects.

1) The state of charge on C_7 at the end of a mains half-cycle is well defined, and is independent of events during that half-cycle.
2) The timing ramp is synchronised to the mains waveform.
3) The BR101 is turned off in a well-defined manner, independent of its holding current.

BR101 alternative

Two suitably rated transistors may be used instead of the BR101 if desired. A BC147/BC157 pair may be used if the resistor in series with C_{10} (R_{10}) is increased to 220Ω However, the anode gate must be capable of being reverse-biased by approximately 40V, so a diode (for example, BA318) must be used in series with the base of the p-n-p transistor. Fig. 3 shows an alternative circuit. The 10kΩ resistor R_1 is used to define the turn-on characteristic.

The diode in Fig. 3 provides an additional temperature coefficient of approximately −2mV/degC in the reference potential for the timing ramp. Assuming, for the sake of simplicity, that the ramp is linear, and that it reaches 40V after 6ms of the mains half-cycle, the value of dV/dt is $(40/6 \times 10^{-3})$V/s. The timing error afforded by the extra V_{BE} drop is thus:

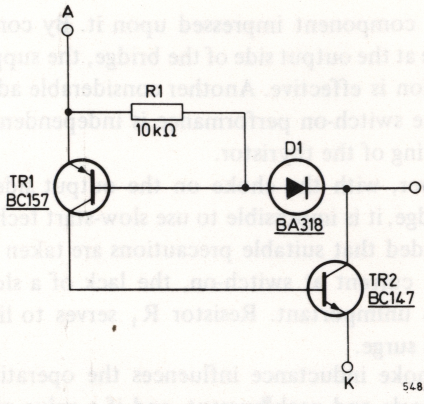

Fig. 3 – BR101 alternative circuit

$$\frac{6 \times 10^{-3} \times 0{\cdot}6}{40} \simeq 10\mu s.$$

During this time the instantaneous value of the mains voltage drops by:

$$240 \times \sqrt{2} \times 100 \times \pi \times \cos(100.\pi.0{\cdot}006) \times 10 \times 10^{-6} \simeq -1V.$$

Therefore, in open loop, this will change the value of output voltage by about −1V; this will be less than 0·1V after feedback is applied. Thus the temperature coefficient effect of the additional diode would be less than 0·1 × (2/600) = 0·3mV/degC at the output of the power supply. This is negligible.

Performance

The stabilisation characteristics of the power supply, together with harmonic distortion measurements, are detailed in Appendix 1. Typically the power supply has an output impedance of about 4Ω, and a mains voltage stabilisation ratio of about 20:1. The ripple voltage is approximately 300mV peak-to-peak at an output current of 800mA.

During the occurrence of appreciable even-order harmonic distortion of the mains supply, the amplitudes of the individual half-cycles may be unequal. Under these conditions, any full-wave power supply with finite loop gain will have a 50Hz ripple voltage at its output because there is a 50Hz component in the full-wave rectified mains waveform. With about 50V peak-to-peak second-harmonic distortion superimposed on the mains waveform, the 50Hz component at the output of the circuit shown in Fig. 2 was about 2V peak-to-peak.

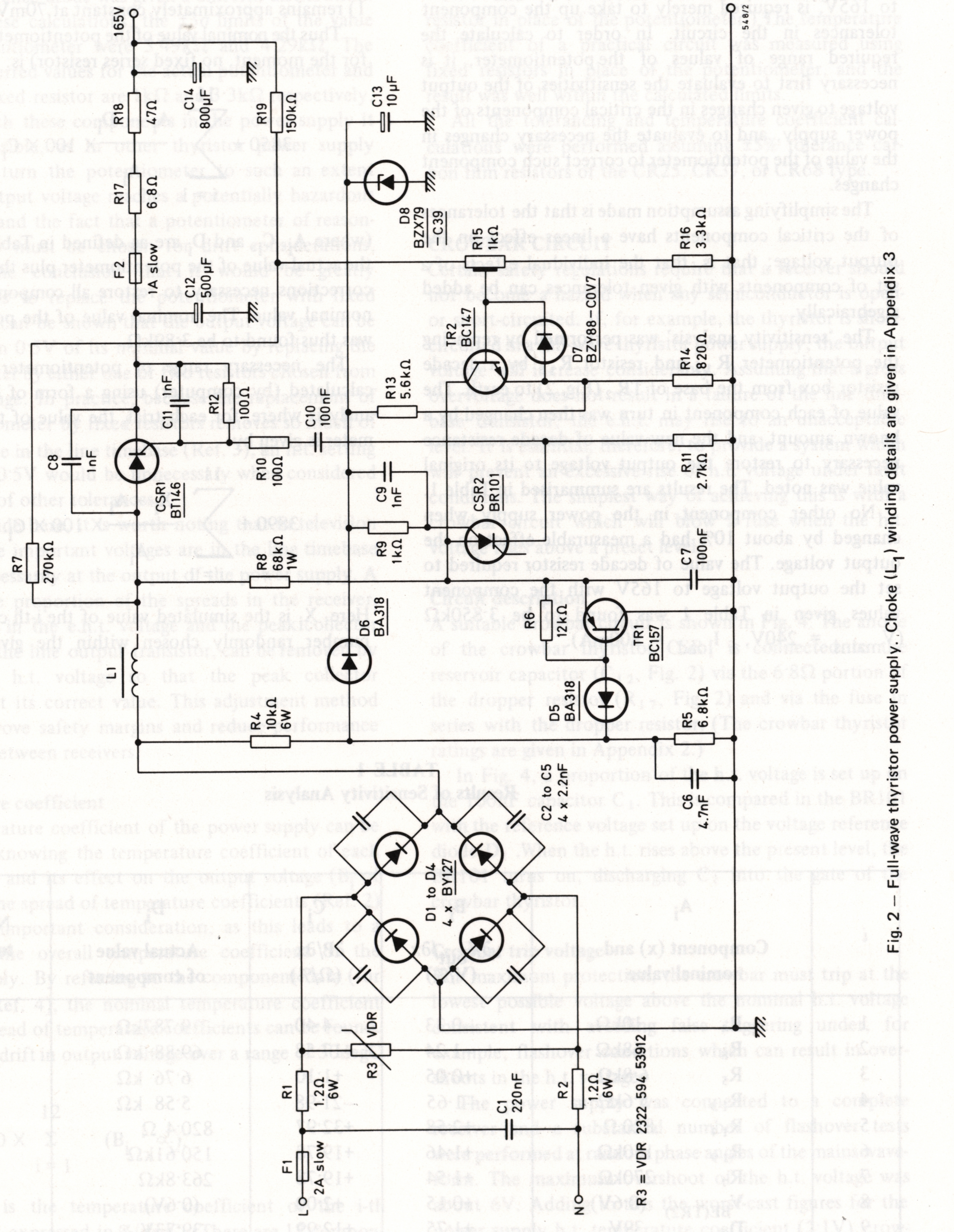

Fig. 2 – Full-wave thyristor power supply. Choke (L_1) winding details are given in Appendix 3

TOLERANCING

Potentiometer tolerancing

The potentiometer R_{15} (Fig. 2), used to set the output to 165V, is required merely to take up the component tolerances in the circuit. In order to calculate the required range of values of the potentiometer, it is necessary first to evaluate the sensitivities of the output voltage to given changes in the critical components of the power supply, and to evaluate the necessary changes in the value of the potentiometer to correct such component changes.

The simplifying assumption made is that the tolerances of the critical components have a linear effect on the output voltage; that is, that the individual effects of a set of components with given tolerances can be added algebraically.

The 'sensitivity analysis' was performed by replacing the potentiometer R_{15} and resistor R_{16} by a decade resistor box from the base of TR_2 (Fig. 2) to earth. The value of each component in turn was then changed by a known amount, and the new value of decade resistance necessary to restore the output voltage to its original value was noted. The results are summarised in Table 1.

No other component in the power supply when changed by about 10% had a measurable effect on the output voltage. The value of decade resistor required to set the output voltage to 165V with the component values given in Table 1 was found to be 3·850kΩ (V_{mains} = 240V, I_{load} = 800mA).

As a check on the measured results in Table 1, it is interesting to note that the rate of change of output voltage with potentiometer value (that is B_i/C_i, see Table 1) remains approximately constant at 70mV/Ω.

Thus the nominal value of the potentiometer (assuming, for the moment, no fixed series resistor) is:

$$3850 + \sum_{i=1}^{11} \frac{A_i - D_i}{A_i} \times 100 \times C_i;$$

(where A_i, C_i, and D_i are as defined in Table 1); that is, the actual value of the potentiometer plus the sum of the corrections necessary to restore all components to their nominal value. The nominal value of the potentiometer was thus found to be 3·89kΩ.

The necessary range of potentiometer values was calculated (by computer) using a form of Monte Carlo analysis where, for each trial, the value of the potentiometer is given by:

$$3890 + \sum_{i=1}^{11} \frac{X_i - A_i}{A_i} \times 100 \times C_i.$$

Here, X_i is the simulated value of the i-th component, a number randomly chosen within the given tolerance range of that component in such a way that, apart from the voltage reference diode, all components have a gaussian distribution about their nominal value. The voltage reference diode was given a uniform distribution.

TABLE 1
Results of Sensitivity Analysis

i	A_i Component (x) and nominal value	B_i $\partial V_{out}/\partial x$ (V/%)	C_i $\partial P/\partial x$ (Ω/%)	D_i Actual value of component	Nominal tolerance (%)
1	R_4 10kΩ	–0·33	–4·40	9·787kΩ	±5
2	R_8 68kΩ	–1·24	–17·58	69·88 kΩ	±5
3	R_5 6·8kΩ	+0·05	+1·10	6·76 kΩ	±5
4	R_{13} 5·6kΩ	–1·65	–21·98	5·58 kΩ	±5
5	R_{14} 820 Ω	+2·58	+32·97	820·4 Ω	±5
6	R_{19} 150kΩ	+1·46	+19·78	150·61kΩ	±5
7	R_7 270kΩ	+1·54	+19·78	263·8kΩ	±5
8	$V_{BE(TR2)}$ (0·6V)	+0·15	+2·00	(0·6V)	±10
9	D_8 39V	+1·75	+12·99	39·73V	±5
10	$R_{17} + R_{18}$ 53·8Ω	–0·01	–0·11	54·49Ω	±5
11	C_7 0·1μF	–0·13	–1·00	0·096μF	±20

From these calculations, the ±3σ limits of the value of the potentiometer were 3·49kΩ and 4·29kΩ. The nearest preferred values for the actual potentiometer and the series fixed resistor are 1kΩ and 3·3kΩ respectively.

Now, with these components in the power supply it will be possible, as in other thyristor power supply designs, to turn the potentiometer to such an extent that the output voltage reaches a potentially hazardous level. This, and the fact that a potentiometer of reasonable quality must be chosen for drift considerations, leads to the conclusion that it would be greatly advantageous to replace the potentiometer with fixed resistors. It can be shown that the output voltage can be set to within 0·5V of its nominal value by replacing the potentiometer by either one or two resistors chosen from the E12 range. In practice, because the replacement of the potentiometer by fixed resistors removes so much of the tolerance in the line timebase (Ref. 3), an h.t. setting to within ±0·5V would be unnecessary when considered in the light of other tolerances.

As an aside here, it is worth noting that in television receivers the important voltages are in the line timebase and not necessarily at the output of the power supply. A considerable proportion of the spreads in the receiver, particularly in the e.h.t. voltage and the peak collector voltage on the line output transistor, can be removed by setting the h.t. voltage so that the peak collector voltage is at its correct value. This adjustment method would improve safety margins and reduce performance variations between receivers.

Temperature coefficient

The temperature coefficient of the power supply can be calculated knowing the temperature coefficient of each component and its effect on the output voltage (B_i of Table 1). The spread of temperature coefficients (Ref. 2) is also an important consideration, as this leads to a spread in the overall temperature coefficient of the power supply. By referring to the component data (for example, Ref. 4), the nominal temperature coefficient and the spread of temperature coefficients can be found. The overall drift in output voltage over a range of 30degC is thus:

$$30 \times \sum_{i=1}^{12} (B_i \cdot \alpha_i),$$

where α_i is the temperature coefficient of the i-th component expressed in %/degC. (There are 12 components now, because the potentiometer must also be considered.) B_i, as above, is the rate of change of output voltage with component value in V/%.

A similar Monte Carlo analysis to that in the previous section was performed, from which the ±3σ limits on the temperature drift over a 30degC range were found to be –1·7V and +2·1V. (This was done assuming a fixed resistor in place of the potentiometer.) The temperature coefficient of a practical circuit was measured using fixed resistors in place of the potentiometer, and the result was well within the calculated limits.

All the tolerancing and temperature coefficient calculations were performed assuming ±5% tolerance carbon film resistors of the CR25, CR37, or CR68 type.

CROWBAR CIRCUIT

Certain safety regulations require that a receiver should not become a hazard when any semiconductor is open- or short-circuited. If, for example, the thyristor is short-circuited in a full-wave thyristor power supply, the output voltage will increase considerably. Assuming that a gross overvoltage does not result in a failure of the line timebase transistor, the e.h.t. may rise to an unacceptable level. It is essential, therefore, to provide a system which will prevent an excessive rise of h.t. voltage under fault conditions. The simplest way of achieving this is with a crowbar circuit which will blow a fuse when the h.t. voltage rises above a preset level.

Circuit description

A suitable crowbar circuit is shown in Fig. 4. The anode of the crowbar thyristor CSR_1 is connected to the reservoir capacitor (C_{12}, Fig. 2) via the 6·8Ω portion of the dropper resistor (R_{17}, Fig. 2) and via the fuse in series with the dropper resistor. (The crowbar thyristor ratings are given in Appendix 2.)

In Fig. 4, a proportion of the h.t. voltage is set up on the 100nF capacitor C_1. This is compared in the BR101 with the reference voltage set up on the voltage reference diode D_1 .When the h.t. rises above the present level, the BR101 turns on, discharging C_1 into the gate of the crowbar thyristor.

Crowbar trip voltage

For maximum protection, the crowbar must trip at the lowest possible voltage above the nominal h.t. voltage consistent with avoiding false triggering under, for example, flashover conditions which can result in overshoots in the h.t. voltage.

The power supply was connected to a complete receiver and a substantial number of flashover tests were performed at random phase angles of the mains waveform. The maximum overshoot of the h.t. voltage was about 6V. Adding to this the worst-cast figures for the power supply h.t. temperature coefficient (2·1V), crowbar temperature coefficient (0·7V), crowbar setting error (0·5V), h.t. setting error (5V assuming 3% for combined meter inaccuracy and reading inaccuracy), and an allowance for drift, the crowbar nominal trip voltage should be 20V above the nominal value of h.t. voltage. The safety margin against false triggering can, of course, be improved by setting the crowbar trip voltage with the same meter (either on the h.t. voltage or on the peak collector voltage of the line output transistor) as that used for setting the h.t. voltage, and by using a digital meter.

Thus, for a nominal h.t. of 165V, the crowbar trip voltage should be 185V (or for a nominal peak collector voltage on the line output transistor of, say, 1200V, the crowbar trip voltage should correspond to 1350V).

Crowbar circuit tolerancing

At an increased h.t. value of 185V, the potentiometer R_4 in the crowbar circuit should be adjustable so that the BR101 can be set just on the point of triggering for all conditions of tolerance on the resistors and the voltage reference diode.

First it is necessary to consider the heating effect of the current flowing through the voltage reference diode. For a diode of nominal voltage V, with a current I flowing through it, the power is:

$$P = V \times I,$$

and the temperature rise is:

$$\Delta T = P \times R_{th} = V \times I \times R_{th}$$

Thus, the change in reference voltage is:

$$\Delta V = \Delta T \times S_z = V \times I \times R_{th} \times S_z;$$

(S_z is the temperature coefficient in V/degC).

Thus, the static slope resistance is:

$$R_{stat} = \frac{\Delta V}{I} = V \times R_{th} \times S_z.$$

The thermal resistance and temperature coefficient of the BZX79–C6V8 are 380degC/W and 4·5mV/degC respectively. Therefore:

$$R_{stat} = 6{\cdot}8 \times 380 \times 4{\cdot}5 \times 10^{-3} \simeq 12\Omega.$$

Therefore, at a current of 1mA, the static resistance effect in a BZX79–C6V8 is negligible. With reference to the data, the dynamic resistance effect of operating at 1mA instead of the 5mA quoted is also negligible.

The BR101 will trip at a gate current of less than 5μA, so the value of V_{GA} will be about 0·5V. The effective series resistance of approximately 12kΩ maximum will add a maximum of 60mV to the trip voltage, referred to the voltage reference diode.

Thus, at zero output current, the voltage at the top of R_4 in Fig. 4, at an h.t. of 185V, should be:

$$V_A > (7{\cdot}2 + 0{\cdot}5 + 0{\cdot}06) = 7{\cdot}76V,$$

and the voltage at the bottom of the potentiometer should be:

$$V_B < (6{\cdot}4 + 0{\cdot}5) = 6{\cdot}9V.$$

Assuming ±5% tolerances for the fixed resistors in the potentiometer chain, and ±20% for the potentiometer itself, the worst-case voltages are:

$$V_A \text{ min} = 7{\cdot}87V,$$

$$V_B \text{ max} = 6{\cdot}20V.$$

Crowbar circuit temperature coefficient

Assuming, as in the rest of the power supply circuit, the use of carbon film resistors throughout, the temperature coefficient effect of the resistors in the crowbar circuit on the trip voltage can be shown to be negligible.

The minimum and maximum temperature coefficients of the BZX79-C6V8 are 1·2 and 4·5mV/degC respectively. Allowing a further –2mV/degC for the anode gate junction of the BR101, the minimum and maximum changes in the crowbar trip voltage (referred to the h.t. rail at 185V) over a 30degC rise in ambient temperature are respectively:

$$30 \times \frac{(1{\cdot}2 - 2)}{10^3} \times \frac{185}{6{\cdot}9} = -0{\cdot}65V,$$

and

$$30 \times \frac{(4{\cdot}5 - 2)}{10^3} \times \frac{185}{6{\cdot}9} = +2V.$$

Crowbar circuit setting procedure

It has been found that the method used for setting the crowbar trip voltage has a substantial effect on the achievable accuracy. The best method of setting the crowbar circuit of Fig. 4 is as follows:

1) Disconnect the anode of the crowbar thyristor CSR_1 (or short-circuit its gate-cathode junction), and set the crowbar potentiometer R_4 to its lowest voltage.
2) Increase the h.t. voltage to 185V (or set the peak collector voltage of the line output transistor to the corresponding increased value). This will be safe provided the receiver is in sync (Ref. 3). If fixed resistors are used in place of an h.t. setting-up potentiometer, a 100kΩ potentiometer can be temporarily connected between chassis and the base of the control transistor.
3) Connect a 20kΩ/V meter, set on the 25V range, with its positive terminal on the voltage reference diode D_1 and its negative terminal on the 100nF capacitor.

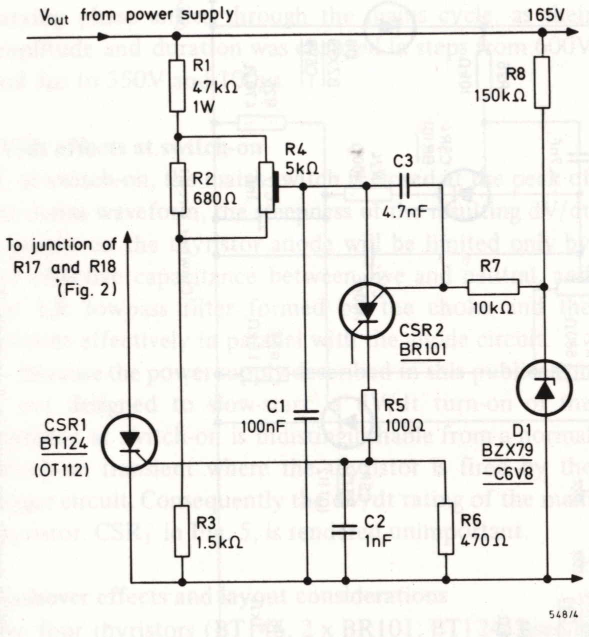

Fig. 4 – Crowbar circuit

4) Carefully adjust R_4 until the trigger circuit just trips. The meter reading will decrease and go through zero as the potentionmeter setting is increased, and will read about -0·5V just before the trip point. When the circuit trips the meter reading will swing to about +5V.
5) Reset the h.t. voltage to its correct value, and reconnect CSR_1.

This method has the advantage that it draws an almost negligible current (about 1μA) from the crowbar trigger circuit at the trip point, thus permitting accurate trip threshold voltage setting. Setting errors of about 0·5V referred to 185V have been achieved in practice without difficulty.

Fuse blowing (due to crowbar operation)

When the crowbar circuit trips, the fuse F_2 at the output of the reservoir capacitor (C_{12}, Fig. 2) is blown, thus protecting the power supply and receiver circuits.

The rate of rise of current in the crowbar thyristor CSR_1 is determined by the combined inductances of the reservoir capacitor, the fuse F_2, the 6·8Ω portion of the dropper resistor, and the associated wiring leading to the anode of the thyristor. In order not to exceed the di/dt rating of the BT124 (50A/μs), the total inductance should be greater than about 4μH.

Several deliberate fuse blowings were performed using Bulgin F283 fuses. The 1A fuse always ruptured in less than 20ms and the peak current was always less than 40A. Knowing the current versus time waveform in the crowbar thyristor, the I^2t value for each case was computed. The $+3\sigma$ limit on the I^2t surge was found to be within the ratings of the BT124 thyristor.

The mains fuse F_1 is normally left intact after operation of the crowbar circuit has ruptured fuse F_2. As the reservoir capacitor (C_{12}, Fig. 2) remains charged even after the mains supply is disconnected, suitable steps must be taken to discharge it before fuse F_2 is replaced.

COMPLETE POWER SUPPLY CIRCUIT

The complete circuit of the 165V power supply and crowbar overvoltage protection circuit is shown in Fig. 5. All forms of power supply must be adequately protected against operational overvoltage and overcurrent effects. In television receivers, these are typically caused by mains supply spike voltages, the effects of picture tube e.h.t. flashover, and switch-on surge currents.

In relation to the circuit of Fig. 5, a large-amplitude mains spike is potentially destructive to the diode bridge or thyristor if it causes their ratings to be exceeded. Both mains spikes and flashover effects can cause false triggering of the main thyristor CSR_1, its control circuit, or the crowbar circuit. Excessive surge currents can flow if the main thyristor is triggered by the high values of dV/dt which can occur on switch-on of the receiver. The following sections describe how adequate protection is provided against these effects.

Mains spikes

Mains spikes can be effectively limited in amplitude to safe levels by the use of a voltage dependent resistor (VDR, type 2322 594 53912). For stability reasons, this device must have no net d.c. component across it, so it must be placed on the mains side of the diode bridge. Spikes were injected into the power supply and the resultant overvoltages were measured. The worst-case reverse spike voltage across the diode bridge was found to be 800V, and the corresponding forward voltage across the thyristor was 600V. (Both these figures allow safety margins in view of the uncertainty of the exact nature of mains spikes.)

It is possible that a very severe mains spike may cause dV/dt triggering of the thyristor, but this is very difficult to enumerate in view of the stated uncertainty of the nature of spikes, particularly of their effective source impedance. It is believed that the 50V/μs rating of the BT146 provides an adequate safety margin.

The ingress of mains spikes to the control circuit can occur via resistor R_4 leading to the base of the p-n-p transistor TR_1, via R_7 to the base of the n-p-n transistor TR_2, and via R_8 to the timing capacitor C_7. The latter two are effectively attenuated by the LR lowpass filter formed by L_1 and resistors R_7 and R_8. A 4·7nF capacitor C_6 provides attenuation of the spike reaching the base of the p-n-p transistor. The power supply was virtually unaffected by repetitive trains of pulses, applied at

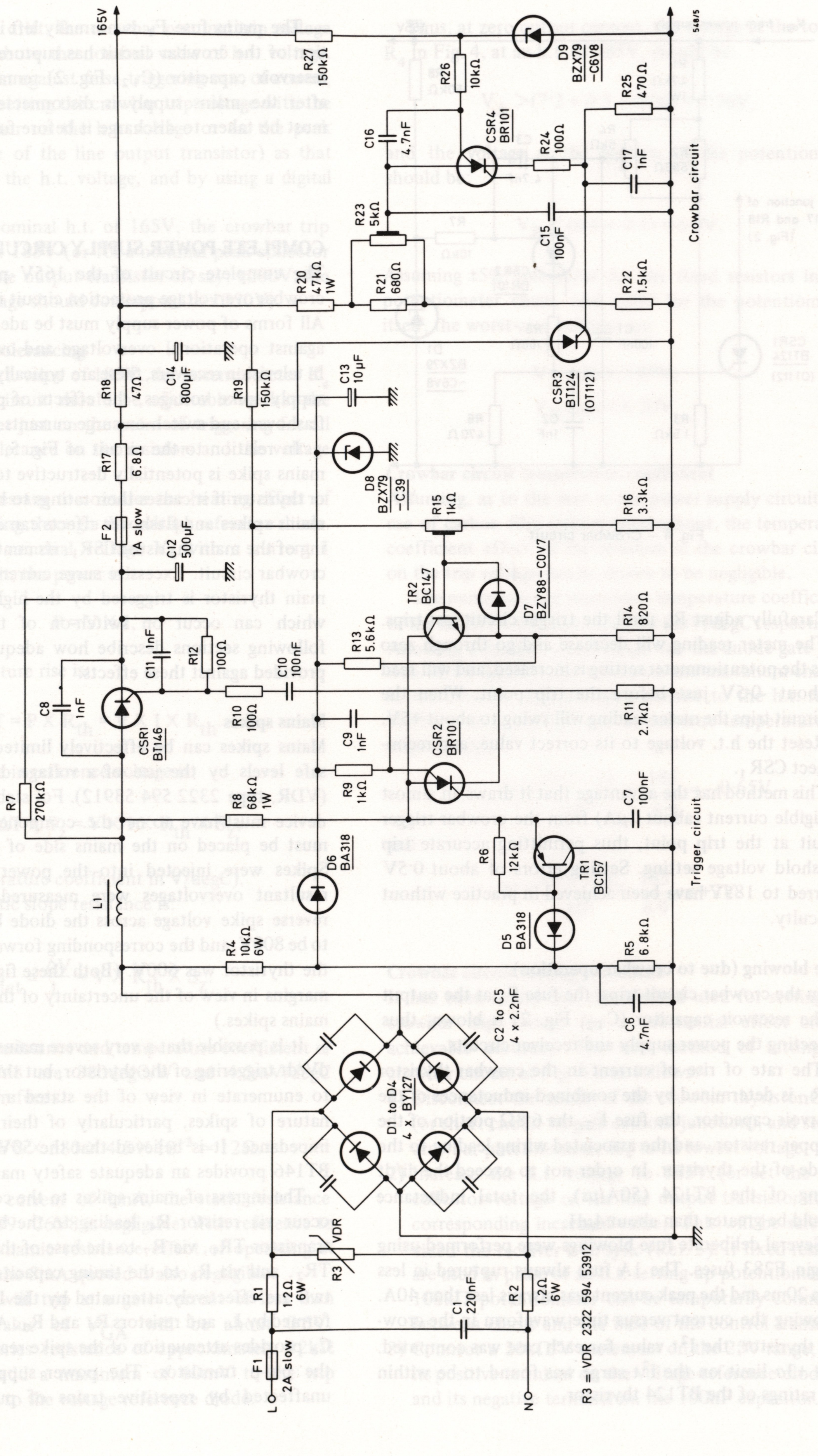
165V
R27 150kΩ
D9 BZX79 –C6V8
R26 10kΩ
R25 470Ω
C16 4.7nF
CSR4 BR101
R24 100Ω
C17 1nF
Crowbar circuit
R23 5kΩ
C15 100nF
R20 47kΩ 1W
R21 680Ω
R22 1.5kΩ
R18 47Ω
C14 800μF
R19 150kΩ
C13 10μF
CSR3 BT124 (OT112)
R17 6.8Ω
D8 BZX79 –C39
R15 1kΩ
R16 3.3kΩ
F2 1A slow
C12 500μF
TR2 BC147
D7 BZY88–C0V7
R14 820Ω
C11 1nF
R12 100Ω
R13 5.6kΩ
C10 100nF
R11 2.7kΩ
C8 1nF
CSR1 BT146
R10 100Ω
C9 1nF
CSR2 BR101
C7 100nF
R7 270kΩ
R8 68kΩ 1W
R9 1kΩ
R6 12kΩ
TR1 BC157
Trigger circuit
D6 BA318
L1
D5 BA318
R5 6.8kΩ
R4 10kΩ 6W
C2 to C5 4 x 2.2nF
C6 4.7nF
D1 to D4 4 x BY127
VDR
R1 12Ω 6W
R2 12Ω 6W
C1 220nF
F1 2A slow
L
N
R3 VDR 2322 594 53912
548/5

Fig. 5 – Full-wave thyristor power supply with crowbar protection circuit. Choke (L1) winding details are given in Appendix 3.

varying phase angles through the mains cycle, as their amplitude and duration was changed in steps from 600V and 3μs to 350V and 100μs.

dV/dt effects at switch-on

If, at switch-on, the mains switch is closed at the peak of the mains waveform, the steepness of the resulting dV/dt transient on the thyristor anode will be limited only by the effective capacitance between live and neutral, and the LR lowpass filter formed by the choke and the resistors effectively in parallel with the anode circuit.

Because the power supply described in this publication is not designed to slow-start, a dV/dt turn-on of the thyristor at switch-on is indistinguishable from a normal switch-on transient where the thyristor is fired by the trigger circuit. Consequently the dV/dt rating of the main thyristor, CSR_1 in Fig. 5, is rendered unimportant.

Flashover effects and layout considerations

The four thyristors (BT146, 2 x BR101, BT124) used in the power supply and crowbar circuit are protected against false triggering under flashover conditions by several small capacitors (C_8, C_9, C_{11}, C_{16}, and C_{17}, in Fig. 5).

The earthing arrangement used in connecting up the power supply is important both in terms of flashover pick-up and the potential differences existing across lengths of wire due to ripple currents.

One arrangement which has been used successfully in flashover tests is illustrated in Fig. 6 and may be summarised as follows.

1) One connection only is made between the negative output of the diode bridge and the negative terminal of the reservoir capacitor (A).
2) One connection only is made between the negative rail of the control circuit and the negative terminal of the reservoir capacitor (B).
3) The negative terminals of the reservoir and the smoothing capacitors are connected together (C).
4) The negative terminal of the smoothing capacitor is finally connected to a central earthing point for the line timebase (D).

The best arrangement found for the connection of the crowbar circuit was a (twisted) pair of wires connecting the crowbar circuit and the two terminals of the smoothing capacitor. All conductors should be kept as short as is reasonable, and any 'flow' and 'return' connections should run along the same path so as to minimise possible induced voltages under transient conditions.

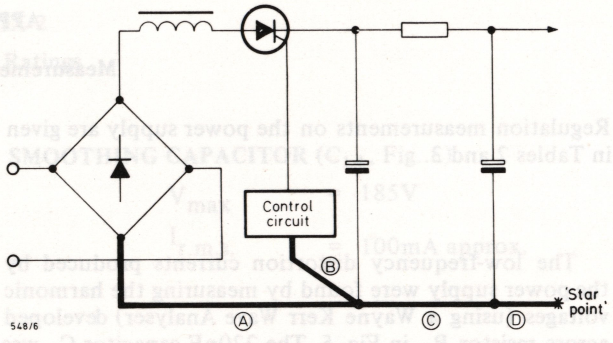
Control circuit
Ⓐ
Ⓑ
Ⓒ
Ⓓ
'Star point'
548/6

Fig. 6 – A possible earthing arrangement

INTERFERENCE

Any rectifier circuit can modulate the r.f. field pattern of the local u.h.f. signal as the diodes alternate between the conduction and off state. This can result in a visible interference pattern on the picture in sync with the mains waveform, particularly when a set-top aerial is used. The simplest cure for this is to physically separate the tuner and i.f. stages from the power supply components and wiring, and to provide an r.f. bypass across each diode, using suitable capacitors.

'FLOATING' CHASSIS

This power supply has a 'floating' chassis connection, so that regardless of the polarity of its connection to the mains supply, the chassis of the receiver is always potentially lethal. The use of a suitable isolating transformer for servicing operations on the receiver is therefore mandatory.

REFERENCES

1. 'The limitations of disturbances in electricity supply networks caused by domestic and similar appliances equipped with electronic devices', CENELEC Standard (Draft), July 1974.
2. BUGG, R.E.F., 'Thyristor power supplies for television receivers: design considerations', **Mullard Technical Communications**, Vol. 12, No. 114, April 1972, pages 129 to 144.
3. 'Phase II horizontal deflection circuit and its design principles', **Mullard Technical Communications**, Vol. 13, No. 121, January 1974, pages 31 to 40.
4. 'CR25 resistors', Mullard Technical Handbook, Book 3, Part 1, October 1974.

APPENDIX 1

Measurements on Power Supply

Regulation measurements on the power supply are given in Tables 2 and 3.

The low-frequency distortion currents produced by the power supply were found by measuring the harmonic voltages (using a Wayne Kerr Wave Analyser) developed across resistor R_2 in Fig. 5. The 220nF capacitor C_1 was removed for the measurements, which were performed using a resistive load taking 800mA at an output voltage of 165V. The mains voltage was 230V, and all distortion components on the mains supply itself, without the power supply as load, were more than 50dB below the fundamental.

For the n-th harmonic, the distortion that would be developed across the 'standard' impedance (0·4 + j0·25)Ω at 50Hz is given by (Ref. 1):

$$D_n = 100\, I_n \sqrt{[(0{\cdot}4)^2 + (0{\cdot}25)^2 n^2]} \,/\, V_{mains} \ \%,$$

where I_n is the current measured at the n-th harmonic of mains frequency. The results are given in Table 4, and show that the distortion components produced by the circuit lie within the CENELEC limits.

TABLE 2

Output Voltage as a Function of Mains Voltage

Mains voltage (V)	Output voltage (V)
190	162·5
200	163·7
210	164·4
220	164·3
230	164·9
240	165·0
250	164·9
260	164·8

I_{out} = 800mA

TABLE 3

Output Voltage as a Function of Load Current

Load current (mA)	Output voltage (V)
600	166·4
700	165·6
800	165·0
900	164·4
1000	164·0
1100	164·0

V_{mains} = 240V

TABLE 4

Low-frequency Distortion Components

Harmonic number	Percentage distortion (%)	CENELEC limit (%)
2	0·029	0·20
3	0·410	0·85
4	0·039	0·20
5	0·533	0·65
6	0·032	0·20
7	0·516	0·60
8	0·015	0·20
9	0·370	0·40
10	0·173	0·20
11	0·201	0·40
12	0·037	0·20
13	0·028	0·30
14	0·040	0·20
15	0·129	0·25
16	0·026	0·20
17	0·173	0·25
18	0·012	0·20
19	0·137	0·25
20	0·026	0·20
21	0·054	0·25
22	0·040	0·20
23	0·037	0·25
24	0·035	0·20

APPENDIX 2

Component Ratings

RESERVOIR CAPACITOR

This component (C_{12}, Fig. 5) must be able to withstand peak mains voltage, either transiently at switch-on, or indefinitely at zero current after the crowbar has tripped. Its normal working voltage should be 250V.

Ripple current = 2·2A r.m.s. (6·5A peak-to-peak).

SERIES THYRISTOR (CSR_1, Fig. 5)

V_{RWM} = 400V

V_{RSM} = 400V

V_{DWM} = 150V

V_{DSM} = 600V

$I_{T(AV)}$ = 1A

$I_{T(r.m.s.)}$ = 2·2A

I_{TRM} = 6A

I_{TSM} = 86A, 5ms

dV/dt = 50V/μs

I_{GT} = 100mA

This specification is adequately met by the Mullard BT146 type.

SMOOTHING CAPACITOR (C_{14}, Fig. 5)

V_{max} = 185V

$I_{r.m.s.}$ = 100mA approx.

CROWBAR THYRISTOR (CSR_3, Fig. 5)

V_{RWM} = 0V

V_{RSM} = 0V

V_{DWM} = 250V

V_{DSM} = 400V

$I_{T(AV)}$ = 0A

$I_{T(r.m.s.)}$ = 0A

I_{TRM} = 0A

I_{TSM} = 40A, 10ms

dV/dt = –

I_{GT} = 30mA

This specification is adequately met by the Mullard BT124 type.

APPENDIX 3

Choke Construction

The choke was constructed using an HWR 10/8/13 C-core with two single bobbins.

380 turns (190 per bobbin)

0·8mm wire

Airgap = 5mm (2·5mm per limb).

Flyback converters with current transformer drive

J.R. Kinghorn
Mullard Central Application Laboratory

UDC 621.314.12: 621.314.224

The flyback converters described in this article use current transformer drive for the output transistor bases. The resulting system has several advantages: in particular, a very wide range of input voltages can be accommodated. Practical circuits are given, and construction as a standard module is considered.

INTRODUCTION

The flyback ('ringing-choke') converter system is often used in small power supplies; in its simplest form, however, it suffers from several limitations. In particular, the system has a low efficiency when the design attempts to accommodate wide spreads in transistor parameters and a wide input voltage range.

The use of a current transformer to supply base drive to the output transistor offers a solution to these problems. When current transformer drive is used in conjunction with other modifications described in this article, the resulting system is inherently free from the effects of spreads in output transistor parameters. A more efficient design is achieved, and the system is capable of operating from a very wide range of input voltages with good output voltage stability.

The basic principles of the technique are given in this article and compared with those of the simple flyback system. The new technique is applied to the design of a system providing +5V at 200mA and ±15V at 60mA, from a 6 to 30V supply. The operating frequency of the system described is proportional to the load, and the system is thus more suitable for approximately constant loads. A modification to the system, also described, allows a constant operating frequency for widely varying load currents.

In view of the high efficiency and wide range of permissible input voltages, the system is considered particularly suitable for all types of battery-operated equipment.

CONVENTIONAL FLYBACK CONVERTER

A flyback converter using a very simple method of base drive is shown in Fig.1a. Converter waveforms for two modes of operation are given in Fig.1b. The operation of the system is as follows. Let capacitor C_1 be charged initially to a negative voltage. Current now flows via R_1, and C_1 charges towards $+V_{in}$. When the voltage V_{C1} across C_1 reaches about +0·7V (at time t_1) a small current begins to flow via R_2, and TR_1 starts to turn on. As the collector-emitter voltage V_{CE} of TR_1 starts to fall the voltage across winding (1) of transformer T_1 increases, providing increased base drive. Positive feedback action results, and V_{CE} falls rapidly to the saturation value, $V_{CE(sat)}$. The peak value of the base current i_B at this time is:

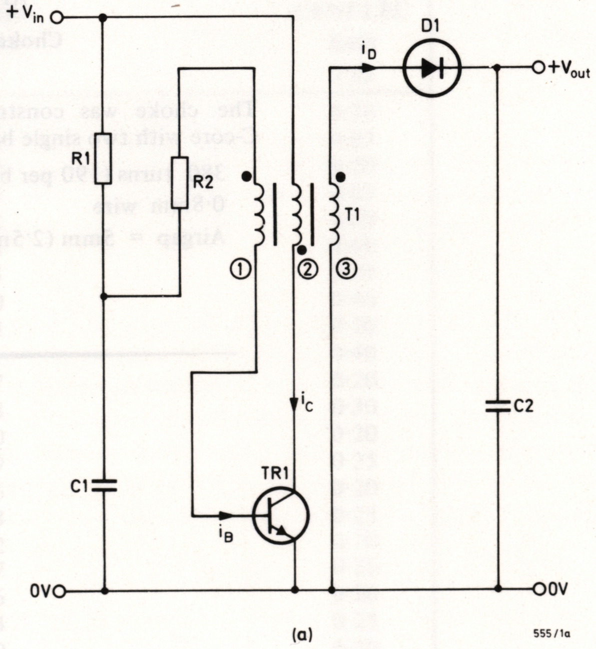

Fig.1a – Conventional flyback converter circuit

$$I_{B(pk)} \simeq \frac{V_{in}}{R_2}\left(\frac{n_1}{n_2}\right),$$

where n_1 and n_2 are the numbers of turns on transformer windings (1) and (2) respectively.

Current now builds up linearly in winding (2) of T_1 according to the relationship:

$$\frac{di_C}{dt} = \frac{V_{in} - V_{CE(sat)}}{L_2},$$

where L_2 is the inductance of winding (2). Meanwhile, the base current i_B decays exponentially with a time-constant of approximately C_1R_2. This process continues until the decreasing base current is no longer sufficient to sustain the increasing collector current (at time t_2). Transistor TR_1 now starts to come out of saturation and, as the collector voltage increases, the voltage across winding (1) of T_1 decreases, providing even less base drive. Positive feedback action again occurs, and i_C rapidly falls to zero.

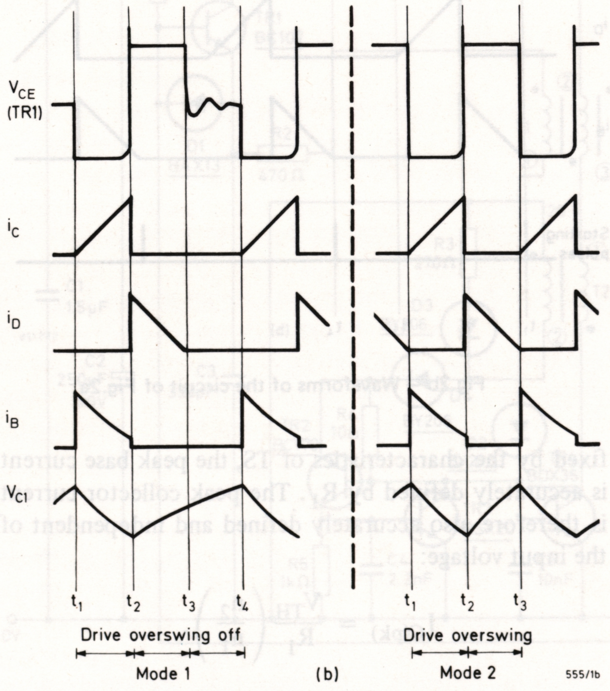

Fig.1b – Waveforms of the circuit of Fig.1a

The stored energy in T_1, that is $\frac{1}{2}L_2(I_{C(pk)})^2$, now causes the voltages across T_1 to reverse, until the voltage of winding (3) is clamped at V_{out} by D_1 (overswing). A linearly decreasing current i_D then flows to charge C_2, where:

$$\frac{di_D}{dt} = \frac{V_{out} + V_{D1}}{L_3}.$$

The value of capacitor C_2 is assumed to be large, so that the ripple voltage across the capacitor is small, and the mean value of i_D averaged over the complete cycle is equal to the output load current.

When i_D has fallen to zero at time t_3, the voltage across T_1 collapses. When operating in mode 1 (Fig.1b), the system then remains in the quiescent state until C_1 has charged sufficiently to turn on TR_1 again at time t_4. The cycle then repeats. Alternatively, capacitor C_1 may already have charged sufficiently at time t_3 to turn on TR_1, in which case operation in mode 2 results.

This method of base drive is very wasteful of power. When TR_1 is first turned on maximum base drive is applied, although it is not needed as the collector current is small. Just before TR_1 is turned off the collector current is at its largest, and yet it is at this time that minimum base current is supplied. This results in a high value of transistor $V_{CE(sat)}$ at the worst possible time, giving high dissipation in TR_1. Power is also wasted in the base drive circuit. Capacitor C_1 is discharged to a negative voltage by the base current when TR_1 is on. If the on-time and off-time of TR_1 are approximately equal, as in most cases they will be, then C_1 must be recharged to the starting voltage in about the same time. The mean base current must therefore flow through R_1 during the off-time of TR_1, and since R_1 is supplied from the full input voltage there may be considerable power loss. In a stabilised system R_1 is normally replaced by part of a feedback amplifier supplied from V_{out}. If V_{out} is of the same order as V_{in} then the system is even less efficient, as the energy for the base drive has to be supplied via the basic conversion efficiency of the inverter.

Another disadvantage of this method of base drive is that the on-time of TR_1 depends on its h_{FE}, as this parameter dictates at what time i_B becomes insufficient to sustain i_C. The peak collector current is therefore not well defined, and if the system is stabilised then the operating frequency is subject to wide tolerances.

Furthermore, if the input voltage changes then there is an equivalent change in peak collector current. If the input voltage doubles, say, then the base drive will also double, allowing twice the original collector current to be sustained at time t_2. At the same time, the collector current increases at twice its original rate. The on-time of TR_1 thus remains approximately constant but the peak collector current doubles and the stored energy in the transformer quadruples.

Improvements to this simple flyback (ringing-choke) system, resulting in the current transformer drive system to be described, have been made with the objects of increasing the power conversion efficiency, reducing the dependence of the operating frequency on the transistor parameters, and enabling the converter to operate satisfactorily with a wide range of input voltages.

CURRENT TRANSFORMER DRIVE

The basic output stage of a flyback converter using current transformer drive is shown in Fig.2a. The primary of the current transformer (winding (1) of T_2) carries the collector current (i_C) of TR_1, and has a small number of turns, n_1. The secondary (2) of T_2 has a larger number of turns (n_2) and supplies base drive to TR_1 via a low-value resistor R_1. A threshold switch, TS, short-circuits point Y to point Z when the voltage between points X and Y exceeds a certain small amount (V_{TH}).

The circuit operates as follows. Suppose starting trigger pulse arrives at the base of TR_1 at time t_1. The transistor turns on, and the collector current i_C is transformed by T_2 to provide a base drive current i_B, where:

$$i_B = i_C\left(\frac{n_1}{n_2}\right).$$

The starting trigger pulse may now be removed. Current builds up in the primary of the main transformer T_1 as before, the voltage across the primary of T_2 being small, that is:

$$V_1 = (V_{BE} + i_B R_1)\left(\frac{n_1}{n_2}\right).$$

As the collector current increases, so does the base drive, until at time t_2 the voltage across R_1 reaches the threshold voltage of TS:

$$V_{TH} = I_{B(pk)} R_1.$$

Base drive is then suddenly cut off, TR_1 turns off rapidly, and the voltage across T_1 overswings, as in the simple system described earlier. When all the stored energy has been extracted from T_1 via D_1, the voltage across T_1 collapses (time t_3). The system then remains in the quiescent state until the next starting pulse arrives at time t_4.

The advantages of this method over the conventional method of base drive now become apparent. First, only the base drive required by TR_1 is actually supplied. For example, the ratio n_2:n_1 may be made 20:1. The base current i_B is then always 1/20 of i_C, regardless of the actual value of i_C, and a low $V_{CE(sat)}$ can be maintained throughout the on-time of TR_1. Second, since V_{TH} is fixed by the characteristics of TS, the peak base current is accurately defined by R_1. The peak collector current is therefore also accurately defined and independent of the input voltage:

$$I_{C(pk)} = \frac{V_{TH}}{R_1}\left(\frac{n_2}{n_1}\right).$$

A third advantage of this method is that it is not necessary to supply power for base drive separately. Base drive power is extracted from the collector circuit of TR_1 and is thus unaffected by changes in input voltage. This avoids the waste of power which occurs at high input voltage in a design using conventional voltage drive. The power supplied by the starting pulse need only be very small, since once TR_1 has started to turn on the system will latch. The power taken from the collector circuit is small. For example, suppose V_{TH} = 0·7V, $V_{BE(sat)}$ = 1·3V, and n_2:n_1 is 20:1. The maximum voltage across the primary of the current transformer is then:

$$(V_{TH} + V_{BE(sat)})\left(\frac{n_1}{n_2}\right) = (0{\cdot}7 + 1{\cdot}3)\left(\frac{1}{20}\right),$$
$$= 0{\cdot}1\text{V},$$

which is small (of the order of a typical $V_{CE(sat)}$).

Because the peak collector current is constant, the stored energy in T_1 at the end of the 'on' period is constant. Therefore, for a stabilised system with constant load power, the frequency will also remain constant regardless of input voltage. The only effect of increased input voltage will be to reduce the time taken to reach $I_{C(pk)}$; the reduction is compensated by an increase in the off-time. As the stored energy and output voltage are both constant, the overswing period remains fixed. The output voltage of the system is thus inherently stable for a constant output load. To compensate for load variations and second-order effects, negative feedback may be applied to vary the frequency of starting pulses.

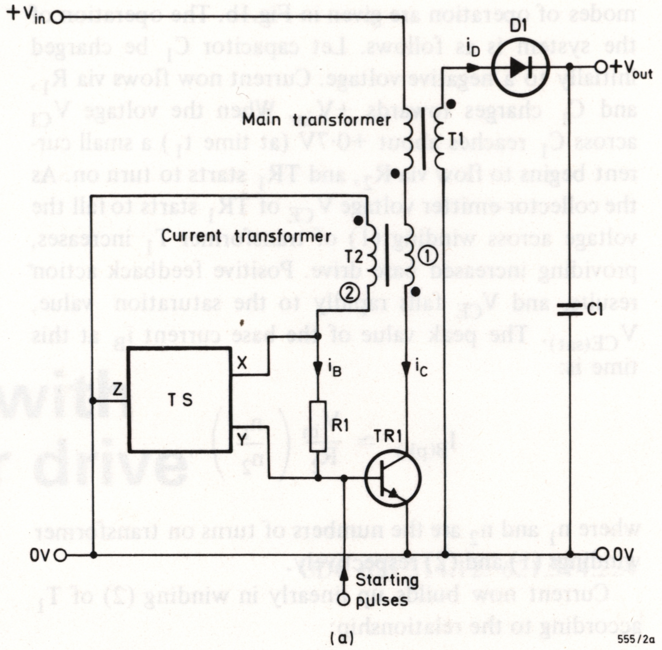

Fig.2a – Basic circuit of flyback converter with current transformer drive

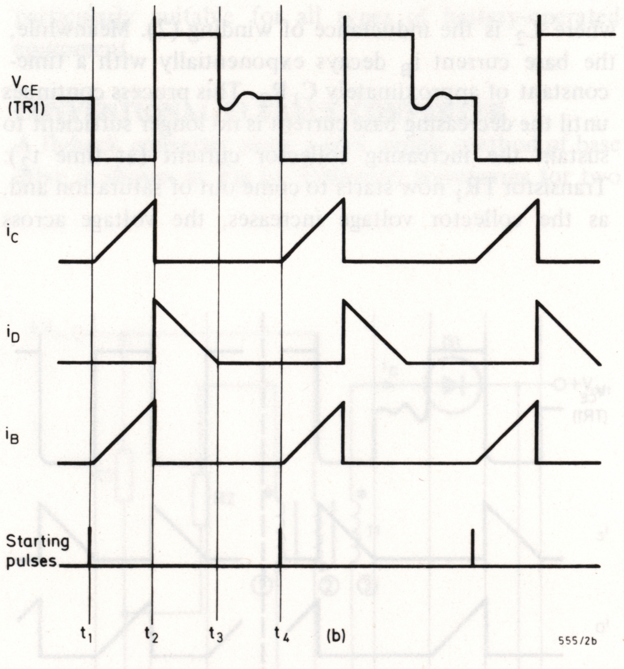

Fig.2b – Waveforms of the circuit of Fig.2a

PRACTICAL SYSTEM DESIGN

The principles outlined above will now be applied to the design of a system with the following specification.

Input voltage	6 to 18V (nominal)
Outputs:	+5V at 200mA
	+15V at 60mA
	−15V at 60mA
Operating frequency	33kHz (nominal)

The complete circuit of a system with this specification is shown in Fig.3. Transistors TR_2 and TR_3 form the threshold switch (TS in Fig.2), and R_4 is the current-sensing resistor. Starting pulses are provided via D_2 by an arrangement very similar to the conventional base drive circuit, but with a smaller current and short time-constant C_3R_2. The charging rate of C_3 is determined by TR_1, which is controlled by feedback from TR_5 and TR_6. The various outputs are provided by windings (3), (4), and (5) on T_1, rectifier diodes D_4 to D_6, and associated reservoir and smoothing capacitors C_6 to C_{12}. The purpose of the choke L_1 is to reduce the ripple voltage on the +5V output.

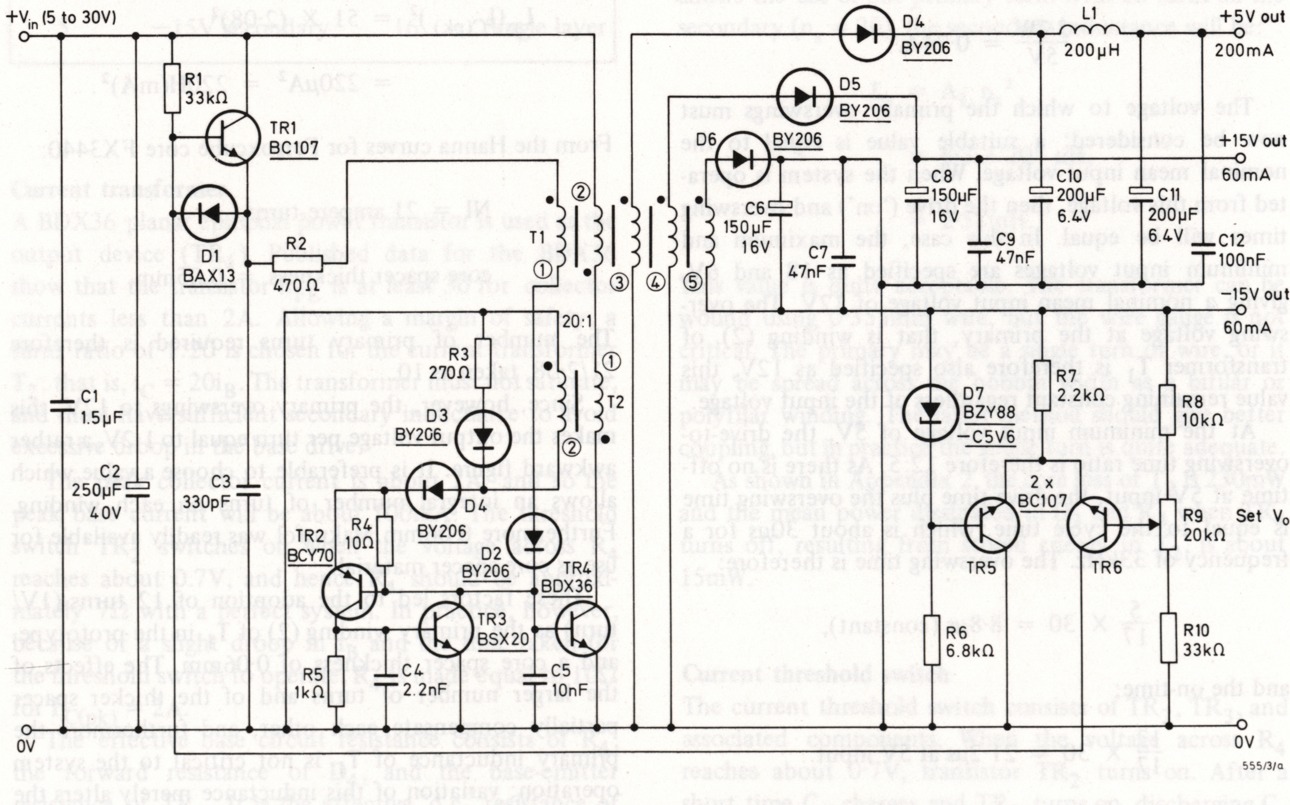

Fig.3 – Practical 3W flyback converter with current transformer drive

The circuit operates as described on page 212 only if the L/R time-constant of the current transformer secondary winding and effective base circuit resistance is long compared with the on-time. If the inductance of the secondary of T_2 is insufficient then the base current will droop relative to the collector current. Also, the small amount of energy stored in T_2 must be removed during the off-time of TR_4: this function is performed by R_3 and D_3, which dissipate the stored energy when the voltage across T_2 reverses.

The design of the system will now be considered.

General system characteristics
The total output power of the system is:

5V, 200mA output	1·0W
2 × 15V, 60mA outputs	1·8W
total	2·8W

Assuming a conversion efficiency of 75%, the input power will be:

$$2{\cdot}8 \times \frac{100}{75} = 3{\cdot}7\text{W}.$$

The minimum specified input voltage is 6V. Allowing for a margin of safety, assume a value of 5V for the input voltage when the off-time disappears and mode 2 operation results (see Fig.1b). The mean input current under these circumstances is:

$$\frac{3{\cdot}7\text{W}}{5\text{V}} = 0{\cdot}74\text{A}.$$

The voltage to which the primary overswings must now be considered: a suitable value is equal to the nominal mean input voltage. When the system is operated from this voltage, then the drive ('on') and overswing times will be equal. In this case, the maximum and minimum input voltages are specified as 18 and 6V, giving a nominal mean input voltage of 12V. The overswing voltage at the primary, that is winding (2), of transformer T_1 is therefore also specified as 12V, this value remaining constant regardless of the input voltage.

At the minimum input voltage of 5V, the drive-to-overswing time ratio is therefore 12:5. As there is no off-time at 5V input, the drive time plus the overswing time is equal to the cycle time, which is about 30µs for a frequency of 33kHz. The overswing time is therefore:

$$\frac{5}{17} \times 30 = 8{\cdot}8\mu\text{s (constant)},$$

and the on-time:

$$\frac{12}{17} \times 30 = 21{\cdot}2\mu\text{s at 5V input.}$$

For a 5V input, the mean collector current during the on-time is therefore:

$$\frac{30}{21{\cdot}2} \times 0{\cdot}74 = 1{\cdot}04\text{A}.$$

The peak collector current is twice this value, that is:

$$I_{C(pk)} = 2{\cdot}08\text{A},$$

and this value remains constant regardless of the input voltage.

Main transformer
It has been shown that, for a 5V input, the collector current must rise from zero to 2·08A in 21·2µs. This parameter determines the primary inductance L_p of the main transformer T_1:

$$L_p = V\frac{dt}{di_C} = 5 \times \frac{21{\cdot}2}{2{\cdot}08},$$

$$= 51\mu\text{H}.$$

A suitable transformer has been designed using the Ferroxcube core FX3440. The following design procedure can, however, be applied to any core size and material suitable for the output power. The FX3440 is an RM8 core in Ferroxcube material A8.

Since the current flow in T_1 is unidirectional, Hanna curves are used to determine the number of primary turns and gap required:

$$L_p(I_{C(pk)})^2 = 51 \times (2{\cdot}08)^2$$

$$= 220\mu\text{A}^2 = 220\text{H(mA)}^2.$$

From the Hanna curves for Ferroxcube core FX3440:

NI = 21 ampere-turns,

core spacer thickness = 0.05mm.

The number of primary turns required is therefore 21/2·08, taken as 10.

Since, however, the primary overswings to 12V, this makes the output voltage per turn equal to 1·2V, a rather awkward figure. It is preferable to choose a value which allows an integral number of turns on each winding. Furthermore 0·06mm Makrofol was readily available for use as core spacer material.

These factors led to the adoption of 12 turns (1V/turn) as the primary winding (2) of T_1 in the prototype, and a core spacer thickness of 0·06mm. The effects of the larger number of turns and of the thicker spacer partially compensate each other, and furthermore the primary inductance of T_1 is not critical to the system operation: variation of this inductance merely alters the operating frequency.

The rest of the design for T_1 follows quite simply. A ratio of 1:3 is suitable for the feedback winding (1), and 1V is allowed for the voltage drop across each secondary rectifier. The number of turns on each winding of T_1 is given in Table 1. All the windings can be wound with 0·355mm enamelled copper wire in single layers with two layers of 0·06mm Makrofol between windings. As mentioned, pieces of 0·06mm Makrofol also form the spacer in the FX3440 core.

Information on flux densities, core losses, and copper losses of this transformer is given in Appendix 1. The total transformer loss is 360mW, an appreciable fraction of the output power. If maximum efficiency is essential, then low-loss core material such as Ferroxcube A9 or A16 is recommended.

TABLE 1
Main Transformer Windings

Winding	Function	Turns	Method
1	Feedback	4	Single layer
2	Primary	12	Single layer
3	+5V secondary	6	Single layer
4	+15V secondary	16	Single layer
5	−15V secondary	16	Single layer

Current transformer
A BDX36 planar epitaxial power transistor is used as the output device (TR_4). Published data for the BDX36 show that the transistor h_{FE} is at least 30 for collector currents less than 2A. Allowing a margin of safety, a turns ratio of 1:20 is chosen for the current transformer T_2; that is, $i_C = 20i_B$. The transformer must not saturate, and must have sufficient secondary inductance to avoid excessive droop in the base drive.

The peak collector current will be about 2A, and so the peak base current will be about 100mA. The threshold switch TR_2 switches on when the voltage across R_4 reaches about 0.7V, and hence R_4 should be approximately 7Ω with a perfect system. In practice, however, because of a slight droop in i_B and the time taken for the threshold switch to operate, R_4 is made equal to 10Ω for $I_{C(pk)} = 2\text{A}$.

The effective base circuit resistance consists of R_4, the forward resistance of D_4, and the base-emitter resistance of TR_4. It is the effective 'd.c.' resistance of D_4 and TR_4 which is important, and not slope resistance, because the ability of the current transformer to sustain a linear current rise depends on the rate of energy loss in the base circuit components. At the mean collector current during the on-time of 1A (i_B = 50mA), the forward voltage drop of D_4 and the V_{BE} of TR_4 are about 0·75 and 1V respectively. The total base circuit resistance is therefore:

$$R = \frac{0{\cdot}75}{0{\cdot}05} + 10 + \frac{1{\cdot}0}{0{\cdot}05},$$

$$= 45\Omega.$$

The maximum on-time, as noted before, is about 22µs. A time-constant ($\tau = L_s/R$) of between two and three times this value, say 50µs, is considered adequate; the secondary inductance of T_2 is then:

$$L_s = R\tau,$$

$$= 45 \times 50\mu\text{H},$$

$$= 2{\cdot}25\text{mH}.$$

A design for the current transformer (T_2 in Fig.3) using the FX3440 core will now be described.

It can be seen from the incremental permeability and Hanna curves for the FX3440 that this core will accept a magnetic field of 2 ampere-turns without a gap. This allows the use of one primary turn. With 20 turns on the secondary (n_s = 20), the secondary inductance will be:

$$L_s = A_L n_s^2,$$

$$= 6{\cdot}3 \times 20^2\ \mu\text{H},$$

$$= 2{\cdot}51\text{mH}.$$

This value is quite acceptable. The transformer can be wound using 0·355mm wire, but the wire gauge is not critical. The primary may be a single turn of wire, or it may be spread across the bobbin width as a bifilar or polyfilar winding. The latter method should give better coupling, but in practice the single turn is quite adequate.

As shown in Appendix 2, the core loss of T_2 is 230mW and the mean power dissipated in D_3 and R_3 when TR_4 turns off, resulting from stored energy in T_2, is about 15mW.

Current threshold switch
The current threshold switch consists of TR_2, TR_3, and associated components. When the voltage across R_4 reaches about 0·7V, transistor TR_2 turns on. After a short time C_4 charges and TR_3 turns on, discharging C_5 and cutting off base drive to TR_4. Capacitor C_4 prevents

spurious noise pulses from operating the switch, and C_5 similarly prevents noise from turning on TR_4. Also, the current switch tends to oscillate at the resonant frequency of T_2: inclusion of C_4 and C_5 entirely prevents this. The transistors TR_2 and TR_3 form in effect a p-n-p-n silicon controlled switch with a high loop gain.

Starting pulse circuit

The starting pulse circuit consists of the feedback secondary on T_1, TR_1, R_2, D_2, C_3, and C_5. The arrangement is very similar to that of the conventional drive circuit described previously. Transistor TR_1 charges first C_3 and then (when D_2 starts to conduct) C_5, until TR_4 turns on slightly. A starting pulse of current is then provided by the feedback voltage across R_2. This current decays rapidly with a time-constant (C_3R_2) of about 150ns which is adequate to allow base drive from the current transformer to come into operation.

The feedback winding may be wound on T_2 instead of T_1. This method is described later.

Negative feedback system

The feedback amplifier is a conventional long-tail pair (TR_5 and TR_6) controlling TR_1. The system is required to be self-starting, and no signal can be supplied from the feedback amplifier until the output voltage rises. When the system is first switched on, resistor R_1 allows TR_1 to charge C_3 at the maximum rate. The output voltage rises, and when it approaches the required level TR_6 starts to conduct. The voltage across R_1 then increases, and C_3 charges less rapidly.

A current of the order of 2mA is supplied to the feedback amplifier by R_7, and a further 1·5mA (approximately) passes through D_7. The feedback amplifier thus consumes less than 55mW from the output of the inverter.

Diode D_1 prevents possible breakdown of TR_1 by limiting the reverse base-emitter voltage to $-0{\cdot}7V$.

For convenience the system is stabilised from the $-15V$ output rail (Fig.3). The other output lines are stabilised by virtue of the turns ratio of T_1, and for good stabilisation there must be tight coupling between the windings on T_1.

If the stability of one of the output voltages of a power supply is particularly critical, then connection of that output to the feedback amplifier is recommended. Positive output voltages can be stabilised if the feedback amplifier is redesigned, but the circuit is more complex if the system is to remain self-starting. To allow all outputs to be floating with reference to the input, it is simplest to provide a separate 'output' winding for stabilisation only.

Output rectification and smoothing

The converter outputs are rectified by diodes D_4 to D_6, and smoothed by capacitors C_6 to C_{12}. Fast rectifiers with low stored charge are, of course, desirable in view of the high edge speeds.

With high-speed systems of this type the inductance of smoothing capacitors becomes significant, and the 'smoothed' output contains a large amount of ripple, including fast spikes. The use of lower-value capacitors with low series inductance in parallel with the main smoothing capacitor is necessary to reduce this ripple, and such an arrangement is shown in Fig.3. Where ripple is still excessive a series inductance can be used. This is the purpose of L_1 in Fig.3, wound with 12 turns of 0·355mm wire on an FX2501 core.

SYSTEM PERFORMANCE

The output voltages, efficiency, and operating frequency of the circuit of Fig.3 are shown as functions of input voltage in Fig.4. They were measured at the full output load of 2·8W.

Operation of the system is possible with input voltages from 5 to 50V, although a fast spike on the collector voltage waveform exceeds the transistor V_{CEO} max. rating (60V) for input voltages above 30V. This spike, which is caused partly by the leakage inductance of T_1 and partly by the turn-on time of the secondary rectifiers, could be limited by clamping the collector overswing voltage to about 14V, using a fast diode. Alternatively, damping components could be connected across T_1 primary, but this method would reduce the converter efficiency.

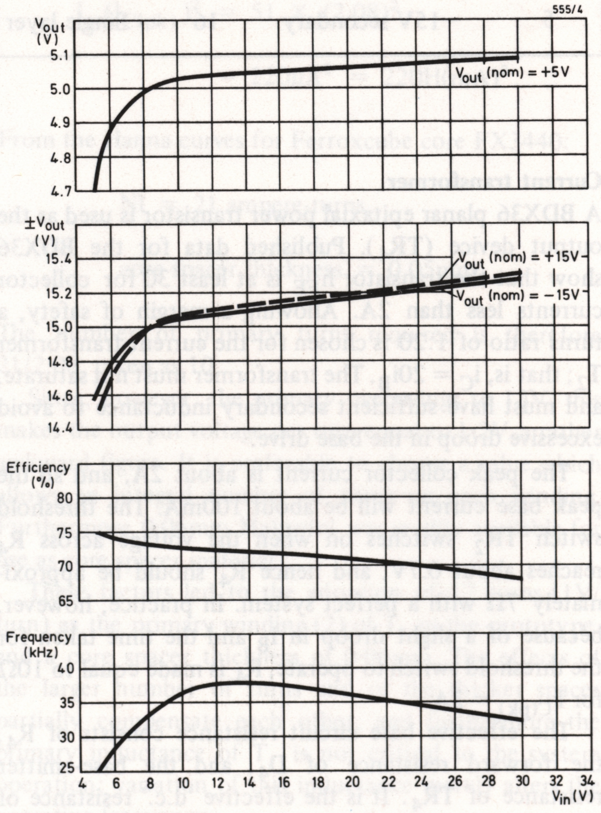

Fig.4 — Performance of the circuit of Fig.3 under constant load

Input voltages below 5V force the frequency downwards into the audible range and regulation is lost. An important feature of the circuit is that the operating frequency remains approximately constant over the whole working range of input voltages.

System losses and regulation

As can be seen from Fig.4, the efficiency of the system falls slightly as the input voltage increases. This behaviour is the reverse of that of conventional converter systems. The reason for the increased efficiency at low input voltages is that in this circuit the base drive is equally effective when the input voltage is low, and $V_{CE(sat)}$ losses do not rapidly increase with decreasing input voltage. (These losses probably do not become significant until a much lower input voltage, perhaps 2V, is reached.) The slight fall in efficiency at higher input voltages is mainly due to an increase in losses in the starting pulse circuit.

At 5V input, a total output power of 2·8W requires an input of 3·74W. The 940mW lost are accounted for approximately as follows

Collector loss

$$\text{Mean collector current} = \tfrac{1}{2} \times 2{\cdot}08 \times \frac{21{\cdot}2}{30},$$

$$= 730 \times 10^{-3}\,\text{A},$$

$$= 730\text{mA};$$

$$V_{CE(sat)} \approx 0{\cdot}05\text{V}.$$

Therefore the loss due to the transistor $V_{CE(sat)}$ is approximately:

$$0{\cdot}05 \times 730 = 37\text{mW}.$$

Base drive loss

Similarly, the voltage across the current transformer primary is approximately:

$$2\text{V} \times \frac{1}{20} = 0{\cdot}1\text{V}.$$

Therefore the base drive loss is:

$$0{\cdot}1 \times 730 = 73\text{mW}.$$

Losses in rectifiers

5V output: $200\text{mA} \times 0{\cdot}6\text{V} = 120\text{mW}$,

15V outputs: $2 \times 60\text{mA} \times 0{\cdot}5\text{V} = 60\text{mW}$.

Main transformer loss

See Appendix 1: 360mW

Current transformer loss

See Appendix 2: 230mW

Feedback amplifier loss

Amplifier supply via R_7 and D_7: 55mW

Total loss

The total loss is therefore: 935mW.

There calculations are merely intended to give a rough indication of the system losses. It can be seen that over 60% of the waste power is lost in the two transformers, mainly as core loss. The use of low-loss core material would probably increase the efficiency of the converter to approximately 85%.

The line regulation is also shown in Fig.4. As can be seen, the regulation of the $-15V$ output is slightly better than that of the other outputs. Nevertheless, all the output voltages vary by less than 5% over the input voltage range from 6 to 30V, and by less than 10% over the range from 5 to 30V.

Load regulation of the system is such that a 10% change in load on an output causes a change of less than 0·3% in that output voltage. In the case of the $-15V$ output, the change is less than 0·1%.

The operating frequency of the system is directly proportional to the total output power. This is a disadvantage in some cases, because when a light load is applied the frequency may fall within the audible range. An alternative method of stabilisation, giving a fixed frequency, is described later.

Peak-to-peak output ripple on each line is about 1% of the output voltage; that is, 50mV on the 5V line and 150mV on the 15V lines. These figures include fast spikes, but they are to some extent dependent on layout and on the particular smoothing components used.

The system oscillates when the input voltage is greater than 2V; voltage and current waveforms of the system under various conditions are shown in Figs.5 to 10.

Since the feedback system responds over one operating cycle, feedback gain can be maintained to quite a high frequency. Ripple rejection is good, and so the system can be operated from mains-derived d.c. which is only roughly smoothed. For example, a 1V peak-to-peak 50Hz sinewave superimposed on a 15V d.c. input results in less than 15mV ripple on the 15V outputs and less than 10mV on the 5V output.

Because the 'output' (overswing) cycle is isolated from the 'drive' cycle, the system is inherently short-circuit proof. The unit may be operated indefinitely into short-circuit loads without damage.

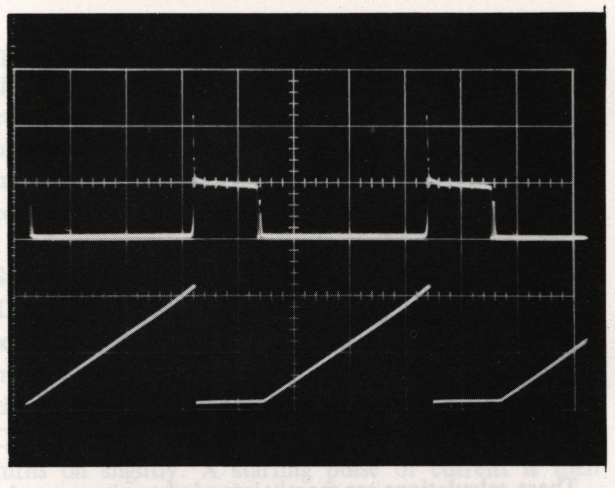

Fig.5 — Collector waveforms: 5V input, full load
Upper trace: collector voltage (20V/main division)
Lower trace: collector current (1A/main division)
Timebase: 10μs/main division

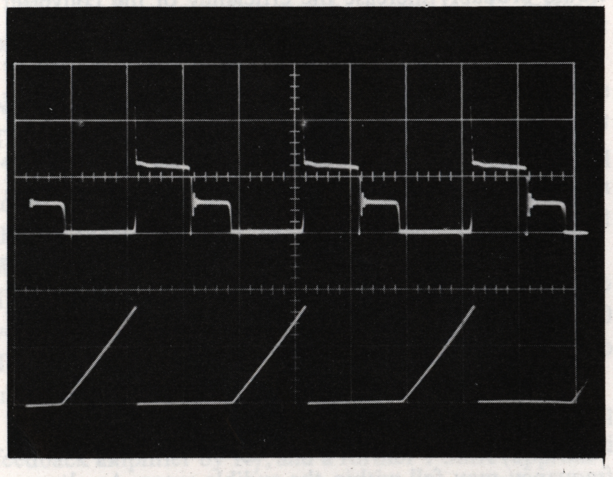

Fig.6 — Collector waveforms: 10V input, full load
Upper trace: collector voltage (20V/main division)
Lower trace: collector current (1A/main division)
Timebase: 10μs/main division

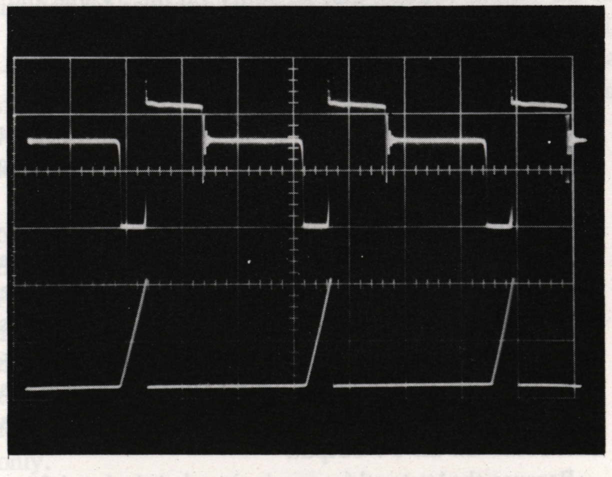

Fig.7 — Collector waveforms: 30V input, full load
Upper trace: collector voltage (20V/main division)
Lower trace: collector current (1A/main division)
Timebase: 10μs/main division

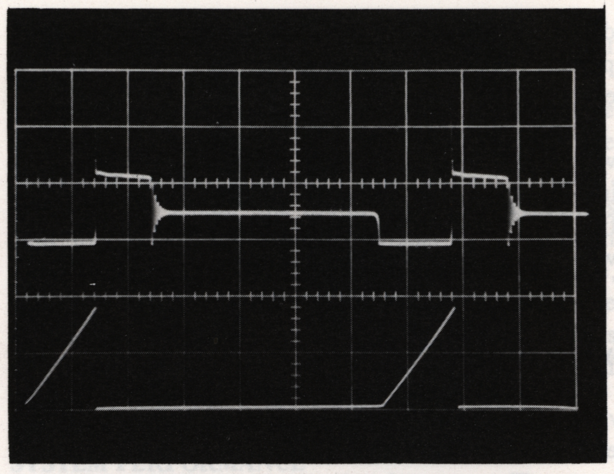

Fig.8 — Collector waveforms: 10V input, half load
Upper trace: collector voltage (20V/main division)
Lower trace: collector current (1A/main division)
Timebase: 10μs/main division

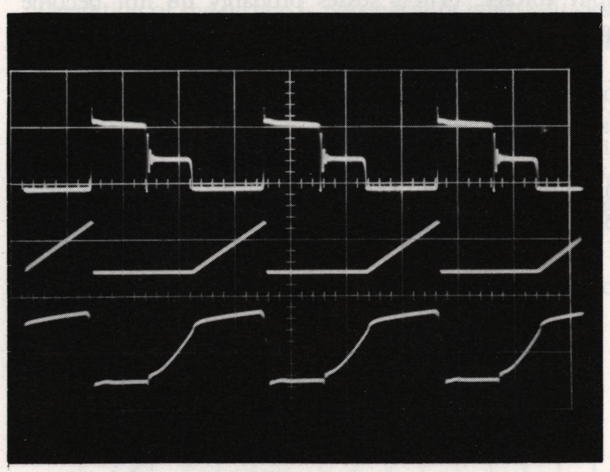

Fig.9 — Collector and base waveforms: 10V input, full load
Upper trace: collector voltage (20V/main division)
Centre trace: collector current (2A/main division)
Lower trace: base voltage (1V/main division)
Timebase: 10μs/main division

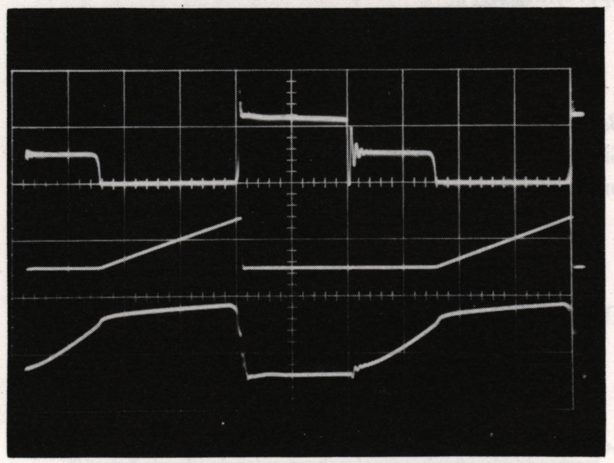

Fig.10 — Collector and base waveforms: 10V input full load
(Traces of Fig.9, expanded)
Timebase: 5μs/main division

MODULAR APPROACH TO THE SYSTEM

The current transformer drive technique is applicable to many small power supply systems, a particular advantage being its operation over a wide range of input voltages. With a few minor modifications the system becomes particularly suitable for construction as a standard module to meet many power supply requirements: such an arrangement is shown in Fig.11.

A standard drive and feedback module, shown within the broken lines in Fig.11, would be used with a separate main transformer. For each application a specially-wound transformer would give the required values of output voltage. Only two windings on the transformer are connected to the module: the primary, and a feedback secondary for output stabilisation.

The operating frequency depends on the output power, the main transformer primary inductance, and the peak collector current determined by R_4. The resistor R_4 would be made externally variable within specified limits so that the operating frequency in any particular case could be brought outside the audible range.

The maximum output power of the module is a function of the minimum input voltage (V_{in} min.) specified by the user, the peak collector current ($I_{C(pk)}$) which is permissible, and the voltage V_{OS} to which the transformer primary overswings. For maximum power transfer, the off-time is designed to be zero when the converter input voltage is V_{in} min., corresponding to converter operation in mode 2. The maximum output power of the module is then given by:

$$P_{out} \text{ max.} = \eta \frac{V_{in} \text{ min. } I_{C(pk)}}{2\left(1 + \dfrac{V_{in} \text{ min}}{V_{OS}}\right)},$$

where η is the overall converter efficiency.

It is evident that the output power may be increased by increasing the overswing voltage V_{OS}. The higher the overswing voltage, the shorter the overswing time, and therefore the on-time may be a higher proportion of the total cycle time. This in turn allows a larger mean input current for a given value of $I_{C(pk)}$. Of course, the maximum overswing voltage that can be used is limited by the V_{CEO} max. rating of TR_4, and the reverse voltage ratings of D_5 and of the output rectifiers. If the drive and overswing voltages are equal (that is, if V_{in} min. = V_{OS}), then the output power is:

$$P_{out} \text{ max.} = \eta \frac{V_{in} \text{ min. } I_{C(pk)}}{4}.$$

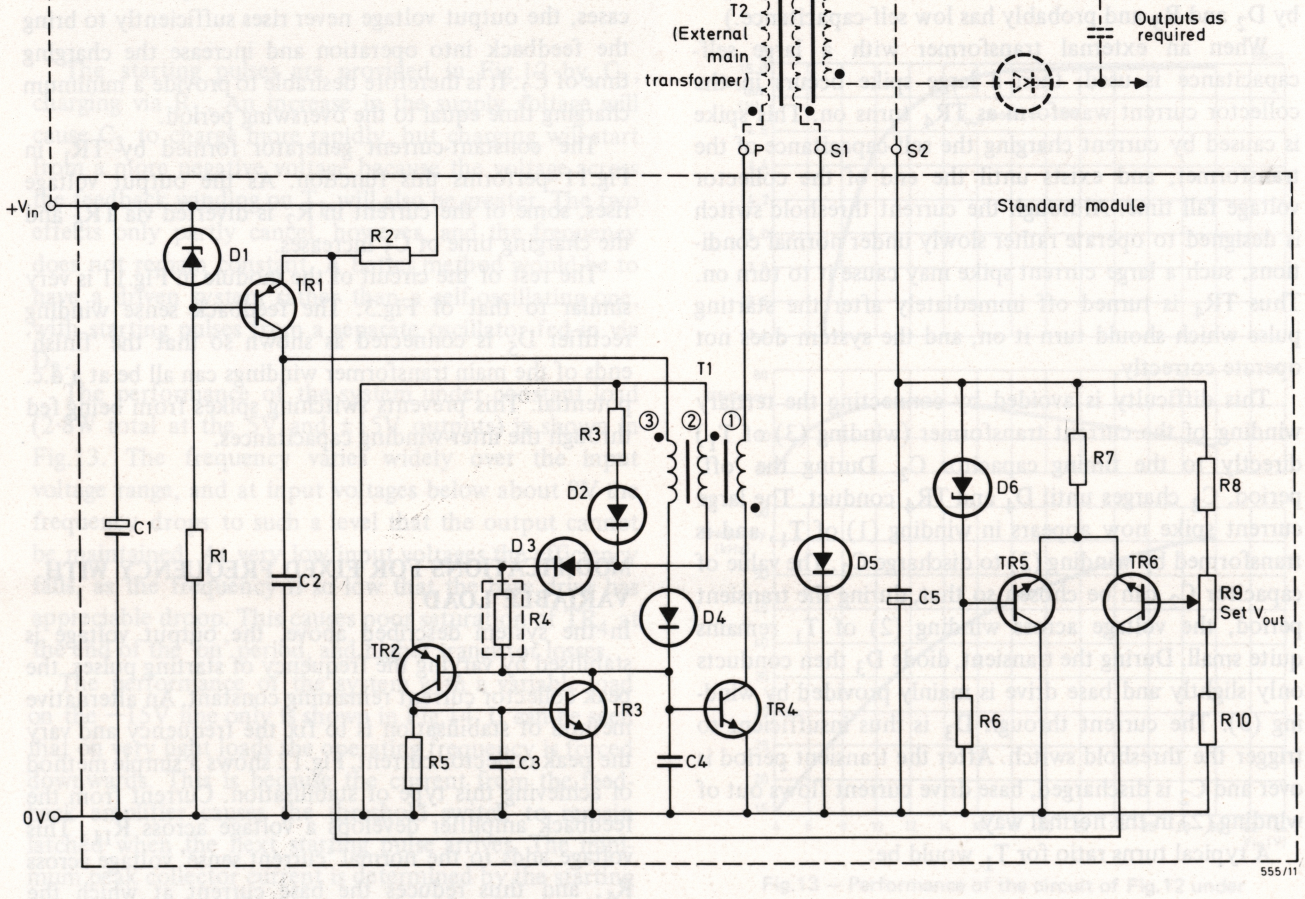

Fig.11 — Modular approach to flyback converter system

The peak collector current is determined by either the I_C max. rating of TR_4, or the current at which transformer T_1 starts to saturate. The minimum input voltage V_{in} min. is specified by the user for a given application, subject to an absolute minimum value for satisfactory operation of the module.

Operation of the module

Feedback for the starting pulses is taken from a tertiary winding on the current transformer T_1, rather than from the main transformer T_2. This reduces the number of external connections on the module to five. A further advantage of obtaining feedback by this method is that the starting pulse circuit is then isolated from the main (external) transformer. If this transformer has an appreciable amount of self-capacitance (reflected across its primary), then ringing will result at the end of the overswing period when the system is quiescent. Damping may be added to remove the ringing, but power is lost in the damping components, and the overall efficiency may drop sharply. It is therefore preferable to isolate the starting pulse circuit from this potential source of ringing, and thus avoid incorrect or erratic modes of operation. (The current transformer, the design of which is within the control of the module designer, is damped by D_2 and R_3 and probably has low self-capacitance.)

When an external transformer with a large self-capacitance is used, then a large spike occurs in the collector current waveform as TR_4 turns on. This spike is caused by current charging the self-capacitance of the transformer, and exists until the end of the collector voltage fall time. Although the current threshold switch is designed to operate rather slowly under normal conditions, such a large current spike may cause it to turn on. Thus TR_4 is turned off immediately after the starting pulse which should turn it on, and the system does not operate correctly.

This difficulty is avoided by connecting the tertiary winding of the current transformer (winding (3) of T_1) directly to the timing capacitor C_2. During the 'off' period, C_2 charges until D_4 and TR_4 conduct. The large current spike now appears in winding (1) of T_1, and is transformed by winding (3) to discharge C_2. The value of capacitor C_2 can be chosen so that, during the transient period, the voltage across winding (2) of T_1 remains quite small. During the transient, diode D_3 then conducts only slightly and base drive is mainly provided by winding (3). The current through D_3 is thus insufficient to trigger the threshold switch. After the transient period is over and C_2 is discharged, base drive current flows out of winding (2) in the normal way.

A typical turns ratio for T_1 would be:

$$n_1:n_2:n_3 = 1:20:40.$$

If this ratio is chosen, then:

1) the peak collector current during the transient spike is limited to the value that can be sustained with a gain of 40 in TR_4;
2) the peak current fed into C_2 during the transient is 1/40 of the peak collector current;
3) capacitor C_2 can discharge through about $(40/20) \times (0{\cdot}7 + 1{\cdot}3) = 4V$ before D_3 begins to conduct and appreciable current flows in winding (2).

These factors allow a suitable value for C_2 to be chosen.

A difficulty arises from the use of the current transformer to provide starting pulses because C_2 always discharges to the same level. When feedback is taken from the main transformer then C_2 discharges to a negative voltage dependent on the input voltage. A charging current dependent on the input voltage will therefore give approximately the same charging time, regardless of input voltage. With the current transformer feedback, however, a constant current is necessary to provide a constant charging time.

If the charging time of C_2 is allowed to become too short when no d.c. feedback signal is applied, then the mode of operation of the system would change during switch-on. Transistor TR_4 then turns on again before the overswing period has finished, and only part of the stored energy available is transferred to the output. In extreme cases, the output voltage never rises sufficiently to bring the feedback into operation and increase the charging time of C_2. It is therefore desirable to provide a minimum charging time equal to the overswing period.

The constant-current generator formed by TR_1 in Fig.11 performs this function. As the output voltage rises, some of the current in R_2 is diverted via TR_6 and the charging time of C_2 increases.

The rest of the circuit of the module in Fig.11 is very similar to that of Fig.3. The feedback sense winding rectifier D_5 is connected as shown so that the 'finish' ends of the main transformer windings can all be at a d.c. potential. This prevents switching spikes from being fed through the inter-winding capacitances.

MODIFICATIONS FOR FIXED FREQUENCY WITH VARIABLE LOAD

In the system described above, the output voltage is stabilised by varying the frequency of starting pulses, the peak collector current remaining constant. An alternative method of stabilisation is to fix the frequency and vary the peak collector current. Fig.12 shows a simple method of achieving this type of stabilisation. Current from the feedback amplifier develops a voltage across R_{11}. This voltage adds to the normal 'current sense' voltage across R_4, and thus reduces the base current at which the threshold switch will turn on.

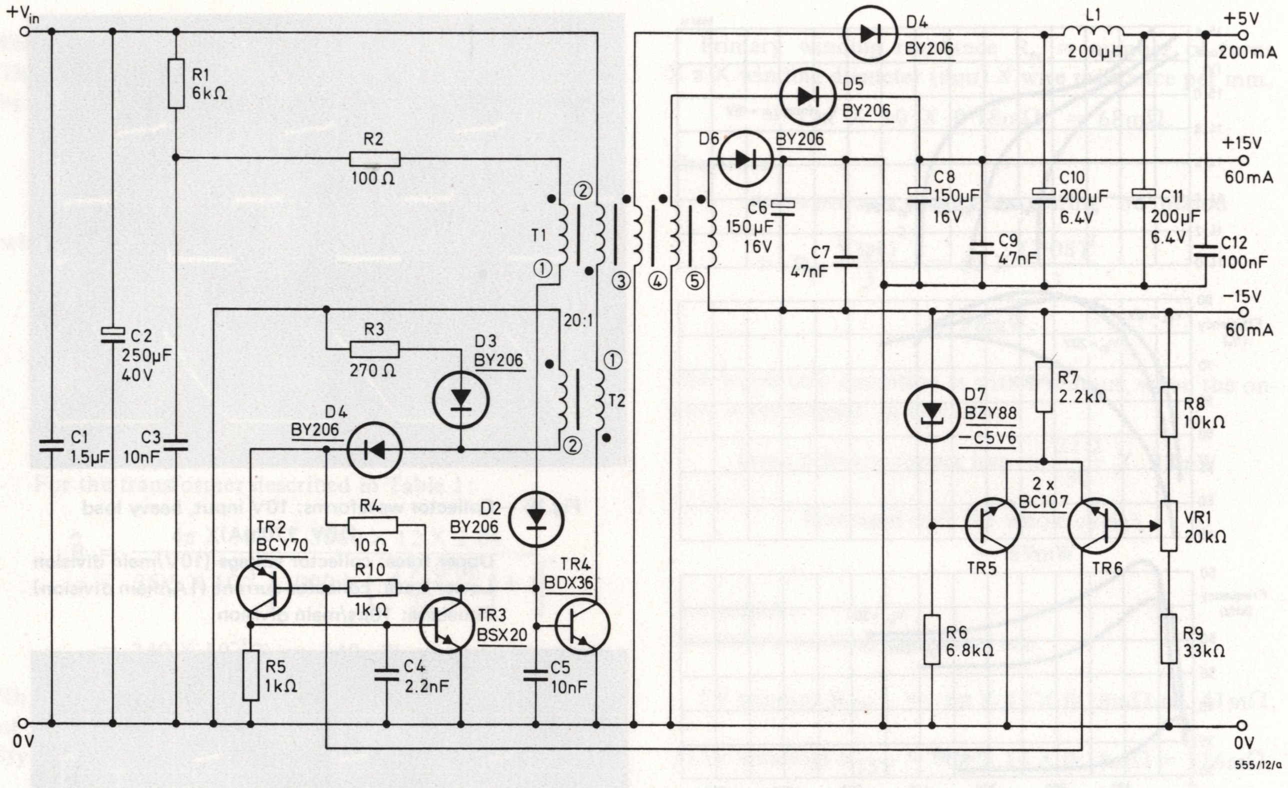

Fig.12 — Flyback converter system of Fig.3, modified to give fixed frequency with variable load

The starting pulses are provided in Fig.12 by C_3, charging via R_1. An increase in the supply voltage will cause C_3 to charge more rapidly, but charging will start from a more negative voltage because the voltage across the feedback winding on T_1 will also be greater. The two effects only partly cancel, however, and the frequency does not remain constant. A better method would be to have a driven system rather than a self-oscillating one, with starting pulses from a separate oscillator fed in via D_2.

The performance of the system under constant load (2·8W total at the 5V and ±15V outputs) is shown in Fig.13. The frequency varies widely over the input voltage range, and at input voltages below about 8V the frequency drops to such a level that the output cannot be maintained. At very low input voltages the efficiency falls, as the frequency is so low that the base drive has appreciable droop. This causes poor saturation of TR_4 at the end of the 'on' period, and higher transistor losses.

The performance of the system with a variable load on the −15V line only is shown in Fig.14. It can be seen that on very light loads the operating frequency is forced downwards. This is because the current from the feedback amplifier causes the threshold switch to remain latched when the next starting pulse arrives. The minimum peak collector current is determined by the starting pulse amplitude and the time taken for the threshold

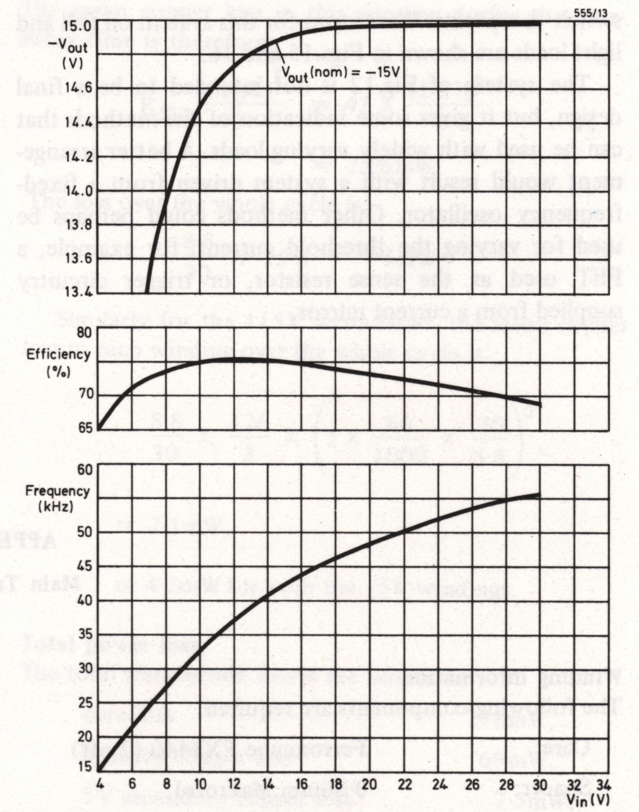

Fig.13 — Performance of the circuit of Fig.12 under constant load

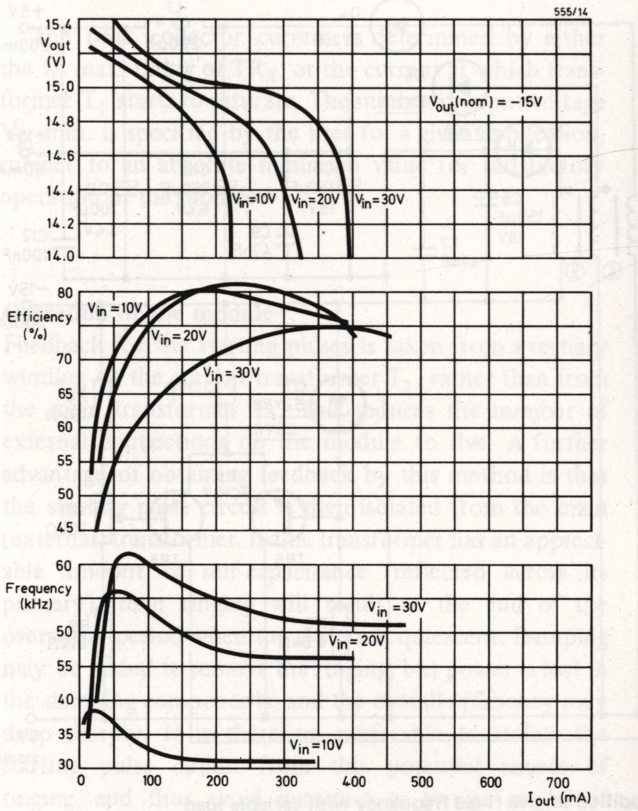

Fig.14 – Performance of the circuit of Fig.12 under variable load

switch to operate. Waveforms for this system on full and light loads are shown in Figs.15 and 16.

The system of Fig.12 is not intended to be a final design, but it gives some indication of the methods that can be used with widely varying loads. A better arrangement would result with a system driven from a fixed-frequency oscillator. Other methods could perhaps be used for varying the threshold current; for example, a FET used as the sense resistor, or trigger circuitry supplied from a current mirror.

APPENDIX 1

Main Transformer

Winding information

The following components are required.

Core:	Ferroxcube FX3440 (2 off)
Spacer:	0·06mm Makrofol
Coil former:	DT2480
Clips:	DT2396 (2 off)

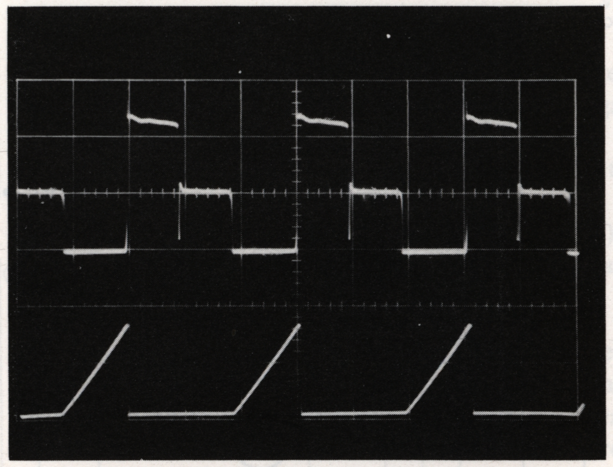

Fig.15 – Collector waveforms: 10V input, heavy load (15V, 170mA)
Upper trace: collector voltage (10V/main division
Lower trace: collector current (1A/main division)
Timebase: 10μs/main division

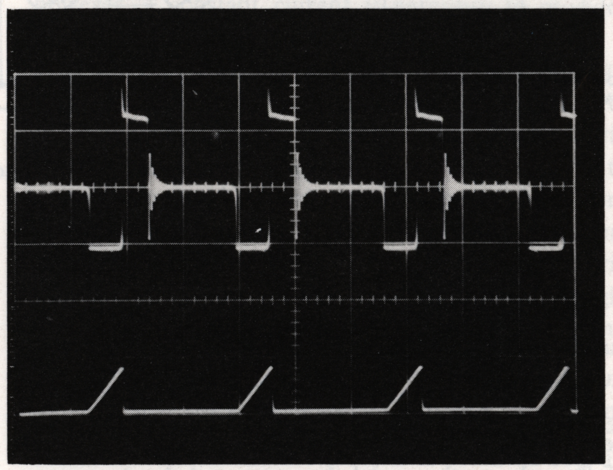

Fig.16 – Collector waveforms: 10V input, light load (15V, 50mA)
Upper trace: collector voltage (10V/main division
Lower trace: collector current (1A/main division)
Timebase: 10μs/main division

Details of each winding are given in Table 1, page 215. All the windings are wound with 0·355mm (29 s.w.g.) enamelled copper wire. The inter-winding insulation consists of two layers of 0·06mm (0·0025in) Makrofol in each case. The start and finish of each winding are marked.

Peak flux density

The peak flux density $\hat{B}$ in the transformer core is given by:

$$\hat{B} = \frac{\mu_o \mu n_p I_{C(pk)}}{\ell_e\left(\mu \dfrac{\ell_g}{\ell_e} + 1\right)}$$

where μ_o is the magnetic constant in SI units;

μ is the (relative) permeability of the core material;

n_p is the number of primary turns;

$I_{C(pk)}$ is the peak transistor collector current;

ℓ_e is the effective magnetic path length; and

ℓ_g is the length of the air gap.

For the transformer described in Table 1:

$$\hat{B} = \frac{4\pi \times 10^{-7} \times 3000 \times 12 \times 2{\cdot}08}{35{\cdot}5 \times 10^{-3}\left[3000 \times \left(\dfrac{2 \times 0{\cdot}06}{35{\cdot}5}\right) + 1\right]},$$

$$= 240 \times 10^{-3}\,\mathrm{T} = 240\mathrm{mT}.$$

This value of $\hat{B}$ is well below the saturation flux density of the Ferroxcube material of the cores, that is, 380mT (typical).

Core loss

The current flow in the transformer is unidirectional, and so the core loss is half the value obtained from power loss density curves. For the material in question, the power loss density (at $\hat{B}$ = 240mT, f = 33kHz, and T_{amb} = 25°C) is approximately 330μW/mm^3.

Thus the core loss in the transformer is:

$$\tfrac{1}{2} \times 300 \times 10^{-6} \times 1850\mathrm{W} = 278\mathrm{mW}.$$

Copper loss

Primary

During the transistor 'on' period the current in the transformer primary rises linearly from zero to $I_{C(pk)}$. If the winding resistance is R_p, then the mean primary copper loss during the 'on' period is given by:

$$\frac{1}{I_{C(pk)}}\int_0^{I_{C(pk)}} R_p\,(i_C)^2\,di_C,$$

$$= \frac{1}{I_{C(pk)}}\left[R_p\,\frac{(i_c)^3}{3}\right]_0^{I_{C(pk)}},$$

$$= \frac{1}{3}\,I_{C(pk)}{}^2 R_p.$$

A similar expression applies to the decay of current in the secondary windings.

The effective winding resistance is taken as equal to the d.c. winding resistance, because the penetration depth at 33kHz is of the same order as the wire diameter.

Primary winding resistance R_p = number of turns × π × winding diameter (mm) × wire resistance per mm,

$$= 12\pi \times 10 \times 0{\cdot}18\mathrm{m\Omega} = 68\mathrm{m\Omega}.$$

Therefore:

mean primary copper loss during 'on' period

$$= R_p\,\frac{I_{C(pk)}{}^2}{3} = 68 \times \frac{(2{\cdot}08)^2}{3},$$

$$= 98\mathrm{mW}.$$

The worst-case condition is with 5V input, when the on-time is the longest. In that case:

$$\text{mean primary copper loss} = \frac{21{\cdot}2}{30} \times 98\mathrm{mW}$$

(averaged over the whole cycle),

$$= 69\mathrm{mW}.$$

Secondaries

Secondary winding resistances are:

5V winding $R_{5V} \approx 6\pi \times 12 \times 0{\cdot}18\mathrm{m\Omega} = 41\mathrm{m\Omega}$;

±15V windings $R_{15V} \approx 16\pi \times 14 \times 0{\cdot}18\mathrm{m\Omega} = 126\mathrm{m\Omega}$.

The current in the 5V winding decays to zero from:

$$I_{5V(pk)} = 2 \times 200 \times \frac{30}{8{\cdot}8}\,\mathrm{mA} = 1{\cdot}37\mathrm{A}.$$

The mean copper loss in this winding during the overswing time is therefore:

$$R_{5V}\,\frac{I_{5V(pk)}{}^2}{3} = 41 \times \frac{(1{\cdot}37)^2}{3},$$

$$= 25{\cdot}6\mathrm{mW}.$$

The loss over the whole cycle is:

$$\frac{8{\cdot}8}{30} \times 25{\cdot}6 = 7{\cdot}5\mathrm{mW}.$$

Similarly for the ±15V secondaries, the mean copper loss in each winding over the whole cycle is:

$$\frac{8{\cdot}8}{30} \times \frac{126}{3} \times \left(2 \times \frac{60}{1000} \times \frac{30}{8{\cdot}8}\right)^2,$$

$$= 2{\cdot}1\mathrm{mW},$$

or 4·2mW for both the 15V windings.

Total power loss

The total transformer loss is the sum of:

core loss	278mW,
primary copper loss	69mW,
5V secondary copper loss	7·5mW,
15V secondaries copper loss	4·2mW;

that is, approximately 360mW.

APPENDIX 2

Current Transformer

Winding information
The following components are required.

Core:	Ferroxcube FX3440 (2 off)
Former:	DT2480
Clips:	DT2396 (2 off)

The primary (1 turn) and secondary (20 turns) are wound with 0·355mm (29 s.w.g.) enamelled copper wire, with several layers of Makrofol as insulation between the windings. The windings occupy only a small amount of the space available, and the primary can be wound using any of several alternative methods given on page 215. The secondary is wound as a single layer. The start and finish of each winding are marked.

Peak flux density
The peak flux density in the transformer core is given by:

$$\hat{B} = \frac{\mu_o \mu n_p I_{C(pk)}}{\ell_e},$$

where the symbols have the same meanings as in Appendix 1.

For this transformer:

$$\hat{B} = \frac{4\pi \times 10^{-7} \times 3000 \times 1 \times 2{\cdot}8}{35{\cdot}5 \times 10^{-3}}$$

$$= 220 \times 10^{-3}\ \mathrm{T} \quad = 220\mathrm{mT}.$$

Core loss
The power loss density for the core at $\hat{B} = 220$mT, f = 33kHz, and $T_{amb} = 25^\circ$C is approximately 250μW/mm³. Therefore the core loss in the transformer is:

$$½ \times 250 \times 10^{-6} \times 1850 = 230\mathrm{mW}.$$

Base current droop
The linear rise of collector current in the transformer primary consists of two components: the transformed secondary current (base drive) and an inductive current. Because of this inductive current there is a droop in the base current. The voltage across the secondary is nearly constant during the 'on' period, and so the rise of the inductive current is approximately linear. The base current therefore also increases linearly, but has a smaller value than that predicted by the transformer turns ratio.

The worst-case condition is when V_{in} = 5V and the transistor on-time is longest (21·2μs). The voltage across the secondary of T_2 varies from approximately 1·7 to 2·7V during this period, having an average of 2·2V. If the secondary inductance is 2·5mH then the inductive current in the secondary at the end of an 'on' period is:

$$\frac{V_s}{L_s} \cdot t_{on} = \frac{2{\cdot}2}{2{\cdot}5 \times 10^{-3}} \times 21{\cdot}2 \times 10^{-6}\ \mathrm{A},$$

$$= 18{\cdot}6\mathrm{mA}.$$

The transformed primary current at this time is (2·08/20) A, that is 104mA, and so the base drive current is only (104–18·6) = 85·4mA. The worst-case droop of base current is thus:

$$\frac{18{\cdot}6}{104} \times 100 = 18\%.$$

The current transformer can be said to have an effective turns ratio of:

$$1{:}20 \times \frac{104}{85{\cdot}4},$$

that is, 1:24 rather than (as wound) 1:20.

The above analysis of base current droop is based on the assumption that the transformer secondary voltage is constant, and is therefore an approximation. The transformer design procedure itself, which assumes that the base circuit resistance is constant, is also approximate. The true base current droop is neither linear nor exponential (as predicted by the above assumptions respectively) but between these extreme conditions. However, because the droop is so small its exact characteristics do not warrant more detailed analysis.

The current transformer secondary inductance is designed so that, when loaded by the effective base circuit resistance, its time-constant is 2 to 3 times the transistor on-time. This is a useful rule-of-thumb which can rapidly be applied to the design of any transformer.

Stored energy
At the end of the 'on' period some energy is stored in the current transformer. This energy is dissipated in diode D_3 and resistor R_3 when i_c is cut off and the voltage across the transformer overswings.

The stored energy is due to the inductive current at the end of the 'on' period, calculated above to be 18·6, say 19mA.

$$\text{Stored energy} = ½\,\mathrm{LI}^2,$$

$$= ½ \times 2{\cdot}51 \times 10^{-3} \times (0{\cdot}019)^2,$$

$$= 4{\cdot}5 \times 10^{-7}\ \mathrm{J}.$$

This quantity of energy is stored and then dissipated once per cycle. The resultant power loss is therefore:

$$4{\cdot}5 \times 10^{-7} \times 33 \times 10^3\ \mathrm{W},$$

that is, 15mW.

Product Information:

FX3700 series transformer cores and coil formers for SMPS

FEATURES OF THE FX3700 RANGE
The FX3700 series of transformer cores is specifically designed for use in switched-mode power supplies and at present comprises four types: FX3720, FX3730, FX3740, and FX3750. The cores are optimised for worst-case application in push-pull circuits operating at 25kHz and giving 5V d.c. output with mains input. In designing the cores, temperature rise has been restricted to 40degC at an ambient temperature of 60°C, thus allowing a maximum design temperature of 100°C. Under the above conditions, output powers up to 500W are achievable. In more favourable applications, output power can be increased by up to 50%. The cores can, of course, also be used in single-ended circuits.

FX3700 series cores are manufactured from a new ferrite material, A16, which has been developed for applications where transformers are required to handle power at ultrasonic frequencies. The characteristics of the material are optimised to maintain high saturation flux densities at high temperatures. Hysteresis losses are reduced compared with those in earlier materials whilst the Curie temperature is in excess of 200°C. Cores made from A16 (measured in pairs) have high amplitude permeabilities, and in addition high resistivities giving low eddy current losses.

In designing the shape of a core for use in an SMPS, a compromise must be made between conflicting requirements. Ideally, any transformer operating at high flux densities and high frequencies should be completely screened to minimise external fields and radiation. It should also allow ease of winding and termination. These considerations have led to the adoption of a round centre-pole E-core design for the FX3700 series. The design is virtually a pot-core with two sides removed, and combines the advantages of both the pot-core (good shielding giving low external fields) and the U + I core (ease of winding and termination).

By adopting a circular cross-section for the centre pole, the turn length is minimised for a given cross-sectional area, an important consideration in reducing copper losses. Furthermore, the winding is more compact, since bowing is eliminated. Grooves which accept metric studding are provided in the outer poles. These facilitate assembly and mounting, and avoid the need for special clips and attachments. However, other fixing methods can be employed by the user where appropriate.

The geometry of cores in the FX3700 series is shown in Fig.1a, and the dimensions of a fully-wound core are

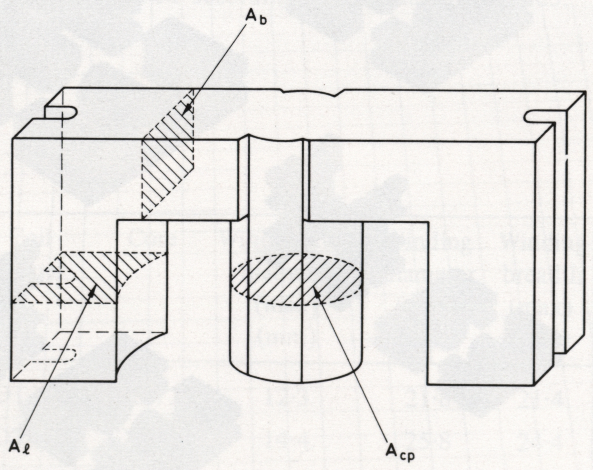

Fig.1a – Dimensions of FX3700 core
(Values are given in Table 1)

shown in Fig.1b. Nominal core dimensions and design data for pairs of cores are given in Table 1.

COIL FORMERS

A range of complementary coil formers, DT2700 series, is available for use with the FX3700 series of cores. The type numbers are set out in Table 2 together with the corresponding core type numbers.

Fig.2 shows the full range of cores with their respective coil formers. Some important features of the coil former design are:

1) Adequate creepage and clearance distances are provided between core and tags to meet the requirements of BS 415 and IEC 65.
2) Positions for up to 16 tags are provided on the two smaller sizes, and for up to 24 tags on the two larger sizes (see Fig.3).
3) A variety of tags with different terminations (for example, wire-wrap, Fast-on*, and solder spill) can be inserted where required.
4) For the two larger coil formers, DT2740 and DT2750, the centre pairs of tag pillars can be removed to allow strip winding terminations to be brought out.

*Registered trademark of Amp (GB) Ltd.

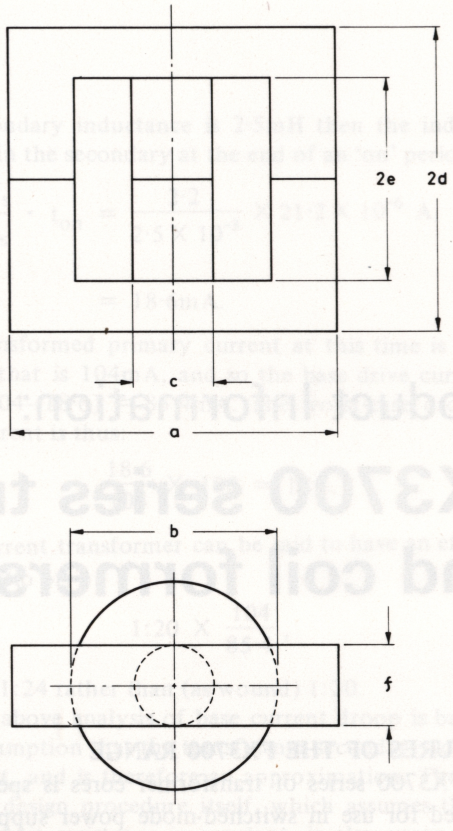

Fig.1b — Dimensions of fully-wound core
(Values are given in Table 1)

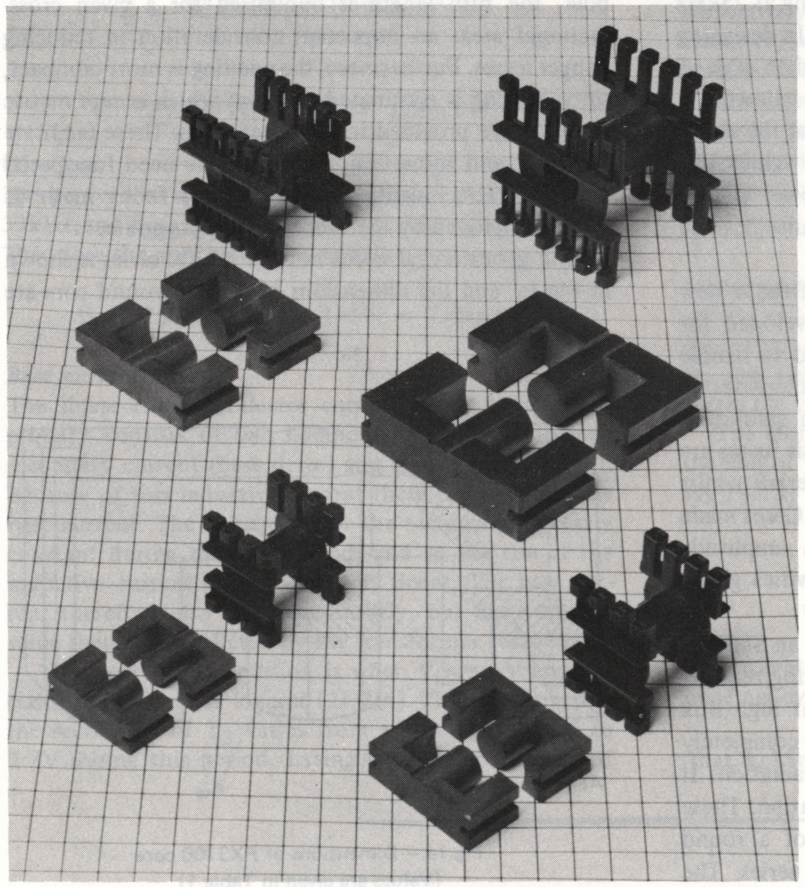

Fig.2 — FX3700 series cores and DT2700 series coil formers (1cm grid). Type numbers of cores and coil formers are set out below as the components appear in the photograph

DT2740 FX3740	DT2750 FX3750
DT2720 FX3720	DT2730 FX3730

TABLE 1

Nominal Dimensions and Design Data for FX3700 Range

	FX3720	FX3730	FX3740	FX3750	Unit
Dimension					
a	34·5	40·6	52·2	70·0	mm
b	22·75	27·05	33·0	44·5	mm
c	9·5	11·6	13·4	16·4	mm
d	17·3	19·5	24·2	34·5	mm
e	12·25	13·9	15·9	22·75	mm
f	9·5	11·6	13·4	16·4	mm
Core details (per pair)					
Total ferrite volume	7780	12600	24300	55600	mm³
Centre pole volume (V_{cp})	1740	2950	4480	9600	mm³
Back and leg volume (V_b)	6040	9650	19820	46000	mm³
Centre pole area (A_{cp})	71·0	106·0	141·0	211·0	mm²
(Minimum centre pole area A_{cp} min)	66·5	100·3	133·8	201·1	mm²
Total back and leg area ($2A_b$)	96·0	130·0	222·0	386·0	mm²
Total surface area of fully-wound core (A_c)	4350	5900	9100	17000	mm²
Mean turn length (ℓ_w)	50·0	60·0	73·0	95·0	mm
Effective parameters					
Magnetic path length (ℓ_e)	76·1	87·9	103	141	mm
Magnetic path area (A_e)	86·5	125	183	283	mm²
Magnetic volume (V_e)	6580	11000	18700	39800	mm³
Core factor (C_1) $\frac{\ell_e}{A_e}$	0·880	0·705	0·562	0·498	mm⁻¹

The effective parameters given above and in published data are calculated according to formulae in IEC 205.

TABLE 2

Coil Former Data

Coil former	Core	Winding tube diameter (max) (mm)	Winding diameter (max) (mm)	Winding breadth (max) (mm)
DT2720	FX3720	12·3	21·8	21·4
DT2730	FX3730	14·4	25·8	24·4
DT2740	FX3740	16·3	31·6	28·2
DT2750	FX3750	19·6	42·7	41·3

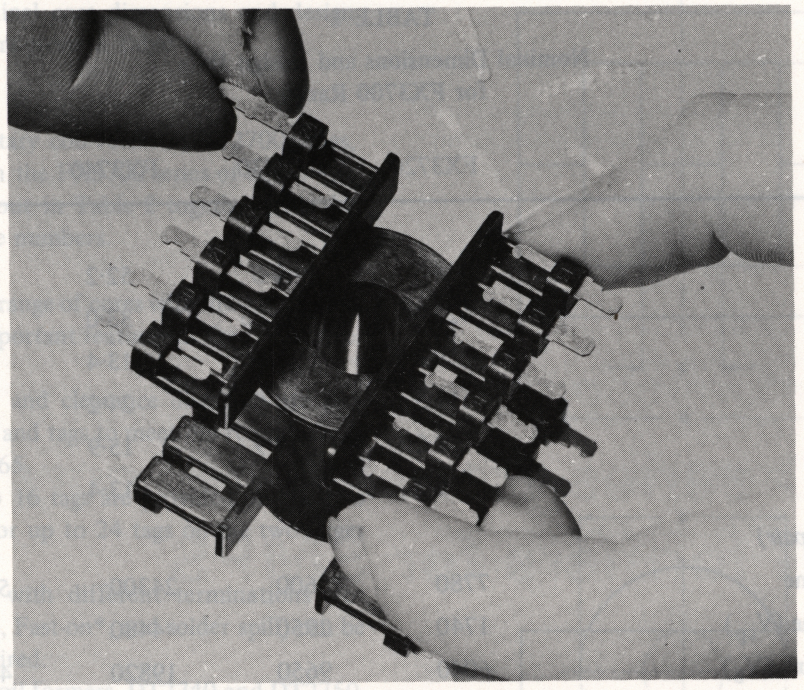

Fig.3 – Insertion of solder tags into coil former

The coil formers are injection moulded in 30% chopped-strand, glass-fibre-loaded Nylon 66 which is coloured black for better heat dissipation. This material has good dimensional stability, is flame retardant, and can be used for continuous operation up to 120°C as specified in BS 2757: 1956, Class E. Tags maintain their positions for normal soldering times and temperatures.

WINDING AREA

The cores and associated coil formers have been designed to give sufficient winding breadth to allow 4mm at each end of the windings for creepage and clearance. This can give 8mm creepage allowance between windings in adjacent layers where required by BS 415 and IEC 65. In addition, the winding depth is large enough to allow the incorporation of insulated screens of 0·1mm copper foil, even with sectionalised windings.

TRANSFORMER DESIGN

Examples of transformer design are given in Refs.1 and 2 together with details on practical winding and assembly. Ref.1 also includes full purchasing information. These publications are available on request.

REFERENCES

1. ‘FX3700 series of transformer cores and coil formers for switched-mode power supplies’, Mullard Limited, 1974, TP1450/1.
2. BARROW, C., ‘Cores for switched-mode power supplies’, **Mullard Technical Communications,** Vol.13, No.124, October 1974, pp.170 to 177. Reprinted as TP1463.